

Information Loss and Power Distortion from Standardizing in Multiple Hypothesis Testing

Luella Fu¹, Bowen Gang², Gareth M. James³, and Wenguang Sun⁴

Abstract

Standardization has been a widely adopted practice in multiple testing, for it takes into account the variability in sampling and makes the test statistics comparable across different study units. However, there can be a significant loss in information from basing hypothesis tests on standardized statistics rather than the full data. We develop a new class of heteroscedasticity-adjusted ranking and thresholding (HART) rules that aim to improve existing methods by simultaneously exploiting commonalities and adjusting heterogeneities among the study units. The main idea of HART is to bypass standardization by directly incorporating both the summary statistic and its variance into the testing procedure. A key message is that the variance structure of the alternative distribution, which is subsumed under standardized statistics, is highly informative and can be exploited to achieve higher power. The proposed HART procedure is shown to be asymptotically valid and optimal for false discovery rate (FDR) control. Our simulation demonstrates that HART achieves substantial power gain over existing methods at the same FDR level. We illustrate the implementation through a microarray analysis of myeloma.

Keywords: covariate-assisted inference; data processing and information loss; false discovery rate; heteroscedasticity; multiple testing with side information; structured multiple testing

¹Department of Mathematics, San Francisco state University .

²Department of Mathematics, University of Southern California.

³Department of Data Sciences and Operations, University of Southern California.

⁴Department of Data Sciences and Operations, University of Southern California.

1 Introduction

In a wide range of modern scientific studies, multiple testing frameworks have been routinely employed by scientists and researchers to identify interesting cases among thousands or even millions of features. A representative sampling of settings where multiple testing has been used include: genetics, for the analysis of gene expression levels (Tusher et al., 2001; Dudoit et al., 2003; Sun and Wei, 2011); astronomy, for the detection of galaxies (Miller et al., 2001); neuro-imaging, for the discovery of differential brain activity (Pacifco et al., 2004; Schwartzman et al., 2008); education, to identify student achievement gaps (Efron, 2008a); data visualization, to find potentially interesting patterns (Zhao et al., 2017); and finance, to evaluate trading strategies (Harvey and Liu, 2015).

The standard practice involves three steps: reduce the data in different study units to a vector of summary statistics; standardize the summary statistics to obtain significance indices such as z -values or p -values; and find a threshold of significance that corrects for multiplicity. Given a summary statistic X_i with associated standard deviation σ_i , traditional multiple testing approaches begin by standardizing the observed data $Z_i = X_i/\sigma_i$, which is then used to compute the p -value based on a problem specific null distribution. Finally, the p -values are ordered, and a threshold is applied to keep the rate of Type I error below a pre-specified level.

Classical approaches concentrated on setting a threshold that controls the family-wise error rate (FWER), using methods such as the Bonferroni correction or Holm’s procedure (Holm, 1979). However, the FWER criterion becomes infeasible once the number of hypotheses under consideration grows into the thousands. The seminal contribution of Benjamini and Hochberg (1995) proposed replacing the FWER by the false discovery rate (FDR) and provided the BH algorithm for choosing a threshold on the ordered p -values which, under certain assumptions, is guaranteed to control the FDR.

While the BH procedure offers a significant improvement over classical approaches, it only controls the FDR at level $(1 - \pi)\alpha$, where π is the proportion of non-nulls, suggesting that its power can be improved by incorporating an adjustment for π into the procedure. Benjamini and Hochberg (2000), Storey (2002) and Genovese and Wasserman (2002) proposed to first estimate the non-null proportion by $\hat{\pi}$ and then run BH at level $\alpha/(1 - \hat{\pi})$.

Efron et al. (2001) proposed the local false discovery rate (Lfdr), which incorporates, in addition to the sparsity parameter π , information about the alternative distribution. Sun and Cai (2007) proved that the z -value optimal procedure is an Lfdr thresholding rule and that this rule uniformly dominates the p -value optimal procedure in Genovese and Wasserman (2002). The key idea is that the shape of the alternative could potentially affect the rejection region but the important structural information is lost when converting the z -value to p -value. For example, when the means of non-null effects are more likely to be positive than negative, then taking this asymmetry of the alternative into account increases the power. However, the sign information is not captured by conventional p -value methods, which only consider information about the null. This work further investigates the usefulness of the configuration of alternative distribution characterized by the variance structure, which has been discarded from standardizing.

Although a wide variety of multiple testing approaches have been proposed, they almost all begin with the standardized data Z_i (or its associated p -value, P_i). In fact, in large-scale studies where the data are collected from intrinsically diverse sources, the standardization step has been upheld as conventional wisdom, for it takes into account the variability of the summary statistics and suppresses the heterogeneity – enabling one to compare multiple study units on an equal footing. For example, in microarray studies Efron et al. (2001) first computes standardized two-sample t -statistics for comparing the gene expression levels across two biological conditions and then converts the t -statistics to z -scores, which are further employed to carry out FDR analyses. Binomial data is also routinely standardized by rescaling the number of successes X_i by the number of trials n_i to obtain success probabilities $\hat{p}_i = X_i/n_i$ and then converting the probabilities to z -scores (Efron, 2008a,b). However, while standardization is an intuitive, and widely adopted, approach, we argue in this paper that there can be a significant loss in information from basing hypothesis tests on Z_i rather than the full data (X_i, σ_i) ¹. This observation, which we formalize later in the paper, is based on the fact that the power of tests can vary significantly as σ changes, but this difference in power is suppressed when the data is standardized and treated as equiva-

¹Unless otherwise stated, the term “full data” specifically refers to the pair (X_i, σ_i) in this article. In practice, the process of deriving the pair (X_i, σ_i) from the original (full) data could also suffer from information loss. This has gone beyond the scope of this work; see the rejoinder of Cai et al. (2019) for related discussions.

lent. In the illustrative example in Section 2.2, we show that by accounting for differences in σ an alternative ordering of rejections can be obtained, allowing one to identify more true positives at the same FDR level.

This article develops a new class of heteroscedasticity-adjusted ranking and thresholding (HART) rules for large-scale multiple testing that aim to improve existing methods by simultaneously exploiting commonalities and adjusting heterogeneities among the study units. The main strategy of HART is to bypass standardization by directly incorporating (X_i, σ_i) into the testing procedure. We adopt a two-step approach. In the first step a new significance index is developed by taking into account the alternative distribution of each X_i conditioned on σ_i ; hence HART avoids power distortion. This kind of conditioning is not possible for standardized values since the σ_i are subsumed under Z_i . Then, in the second step the significance indices are ordered and the smallest ones are rejected up to a given cutoff. We develop theories to show that HART is optimal for integrating the information from both X_i and σ_i . Numerical results are provided to confirm that HART controls the FDR in finite samples and uniformly dominates existing methods in power.

The findings are impactful for three reasons. First, the observation that standardization can be inefficient has broad implications since, due to inherent variabilities or differing sample sizes between study units, standardized tests are commonly applied to large-scale heterogeneous data to make different study units comparable. Second, our finding enriches the recent line of research on multiple testing with side and structural information (e.g. Lei and Fithian, 2018; Cai et al., 2019; Li and Barber, 2019, among others). In contrast with existing works that have focused on the usefulness of sparsity structure, our characterization of the impact of heteroscedasticity, or more concretely *the shape of alternative distribution*, is new. Finally, HART convincingly demonstrates the benefits of leveraging structural information in high-dimensional settings when the number of tests is in the thousands or more. Ideas from HART apply to smaller data sets as well, but the algorithm is designed to capitalize on copious data in ways not possible for procedures intended for moderate amounts of data, and thus is most useful in large-scale testing scenarios where the structure can be learned from data with good precision.

The rest of the paper is organized as follows. Section 2 reviews the standard multiple testing model and provides a motivating example that clearly illustrates the potential power

loss from standardization. Section 3 describes our HART procedure and its theoretical properties. Section 4 contains simulations, and Section 5 demonstrates the method on a microarray study. We conclude the article with a discussion of connections to existing work and open problems. Technical materials and proofs are provided in the Appendix.

2 Problem Formulation and the Issue of Standardizing

This section first describes the problem formulation and then discusses an example to illustrate the key issue.

2.1 Problem formulation

Suppose the summary statistics X_1, \dots, X_m are normal variables obeying distribution

$$X_i | \mu_i, \sigma_i^2 \stackrel{iid}{\sim} N(\mu_i, \sigma_i^2), \quad (2.1)$$

where μ_i follows a mixture model with a point mass at zero and σ_i is drawn from an unspecified prior

$$\mu_i \stackrel{iid}{\sim} (1 - \pi)\delta_0(\cdot) + \pi g_\mu(\cdot), \quad \sigma_i^2 \stackrel{iid}{\sim} g_\sigma(\cdot). \quad (2.2)$$

Here π is the proportion of nonzero signals, $\delta_0(\cdot)$ is a Dirac delta function, and $g_\mu(\cdot)$ and $g_\sigma(\cdot)$ are unknown density functions. Following tradition in dealing with heteroscedasticity problems (e.g. Xie et al., 2012; Weinstein et al., 2018), we assume that σ_i are known. This simplifies the discussion and enables us to focus on key ideas. For practical applications, we use a consistent estimator of σ_i . The goal is to simultaneously test m hypotheses:

$$H_{0,i} : \mu_i = 0 \quad \text{vs.} \quad H_{1,i} : \mu_i \neq 0; \quad i = 1, \dots, m. \quad (2.3)$$

The multiple testing problem (2.3) is concerned with the simultaneous inference of $\boldsymbol{\theta} = \{\theta_i = \mathbb{I}(\mu_i \neq 0) : i = 1, \dots, m\}$, where $\mathbb{I}(\cdot)$ is an indicator function. The decision rule is represented by a binary vector $\boldsymbol{\delta} = (\delta_i : 1 \leq i \leq m) \in \{0, 1\}^m$, where $\delta_i = 1$ means that we reject $H_{0,i}$, and $\delta_i = 0$ means we do not reject $H_{0,i}$. The false discovery rate (FDR)

(Benjamini and Hochberg, 1995), defined as

$$\text{FDR} = E \left[\frac{\sum_i (1 - \theta_i) \delta_i}{\max\{\sum_i \delta_i, 1\}} \right], \quad (2.4)$$

is a widely used error criterion in large-scale testing problems. A closely related criterion is the marginal false discovery rate

$$\text{mFDR} = \frac{E \{\sum_i (1 - \theta_i) \delta_i\}}{E(\sum_i \delta_i)}. \quad (2.5)$$

The mFDR is asymptotically equivalent to the FDR for a general set of decision rules satisfying certain first- and second-order conditions on the number of rejections (Basu et al., 2018), including p -value based tests for independent hypotheses (Genovese and Wasserman, 2002) and weakly dependent hypotheses (Storey et al., 2004). We shall show that our proposed data-driven procedure controls both the FDR and mFDR asymptotically; the main consideration of using the mFDR criterion is to derive optimality theory and facilitate methodological developments.

We use the expected number of true positives $\text{ETP} = E(\sum_{i=1}^m \theta_i \delta_i)$ to evaluate the power of an FDR procedure. Other power measures include the missed discovery rate (MDR, Taylor et al., 2005), average power (Benjamini and Hochberg, 1995; Efron, 2007) and false negative rate or false non-discovery rate (FNR, Genovese and Wasserman, 2002; Sarkar, 2002). Cao et al. (2013) showed that under the monotone likelihood ratio condition (MLRC), maximizing the ETP is equivalent to minimizing the MDR and FNR. The ETP is used in this article because it is intuitive and simplifies the theory. We call a multiple testing procedure *valid* if it controls the FDR at the nominal level and *optimal* if it has the largest ETP among all valid FDR procedures.

The building blocks for conventional multiple testing procedures are standardized statistics such as Z_i or P_i . Let $\mu_i^* = \mu_i / \sigma_i$. The tacit rationale in conventional practice is that the simultaneous inference problem

$$H_{0,i} : \mu_i^* = 0 \quad \text{vs.} \quad H_{1,i} : \mu_i^* \neq 0; \quad i = 1, \dots, m, \quad (2.6)$$

is equivalent to the formulation (2.3); hence the standardization step has no impact on mul-

multiple testing. However, this seemingly plausible argument, which only takes into account the null distribution, fails to consider the change in the structure of the alternative distribution. Next we present an example to illustrate the information loss and power distortion from standardizing.

2.2 Data processing and power loss: an illustrative example

The following diagram describes a data processing approach that is often adopted when performing hypothesis tests:

$$(X_i, \sigma_i) \longrightarrow Z_i = \frac{X_i}{\sigma_i} \longrightarrow P_i = 2\Phi(-|Z_i|). \quad (2.7)$$

We start with the full data consisting of X_i and $\sigma_i^2 = \text{Var}(X_i|\mu_i)$. The data is then standardized, $Z_i = X_i/\sigma_i$, and finally converted to a two-sided p -value, P_i . Typically these p -values are ordered from smallest to largest, a threshold is chosen to control the FDR, and hypotheses with p -values below the threshold are rejected.

Here we present a simple example to illustrate the information loss that can occur at each of these data compression steps. Consider a hypothesis testing setting with $H_{0,i} : \theta_i = 0$ and the data coming from a normal mixture model,

$$X_i|\sigma_i \stackrel{\text{ind}}{\sim} (1 - \pi)N(0, \sigma_i^2) + \pi N(\mu_a, \sigma_i^2), \quad (2.8)$$

where $\sigma_i \sim U[0.5, 4]$, $\mu_a = 2$ and $\pi = P(\theta_i = 1) = 0.1$.

We examine three possible approaches to controlling the FDR at $\alpha = 0.1$. In the p -value approach we reject for all p -values below a given threshold. Note that, when the FDR is exhausted, this is the uniformly most powerful p -value based method (Genovese and Wasserman, 2002), so is superior to, for example, the BH procedure. Alternatively, in the z -value approach we reject for all suitably small $\mathbb{P}(H_0|Z_i)$, which is in turn the most powerful z -value based method (Sun and Cai, 2007). Finally, in the full data approach we reject when $\mathbb{P}(H_0|X_i, \sigma_i)$ is below a certain threshold, which we show later is optimal given X_i and σ_i . In computing the thresholds, we assume that there is an oracle knowing the alternative distribution; the formulas for our theoretical calculations are provided in

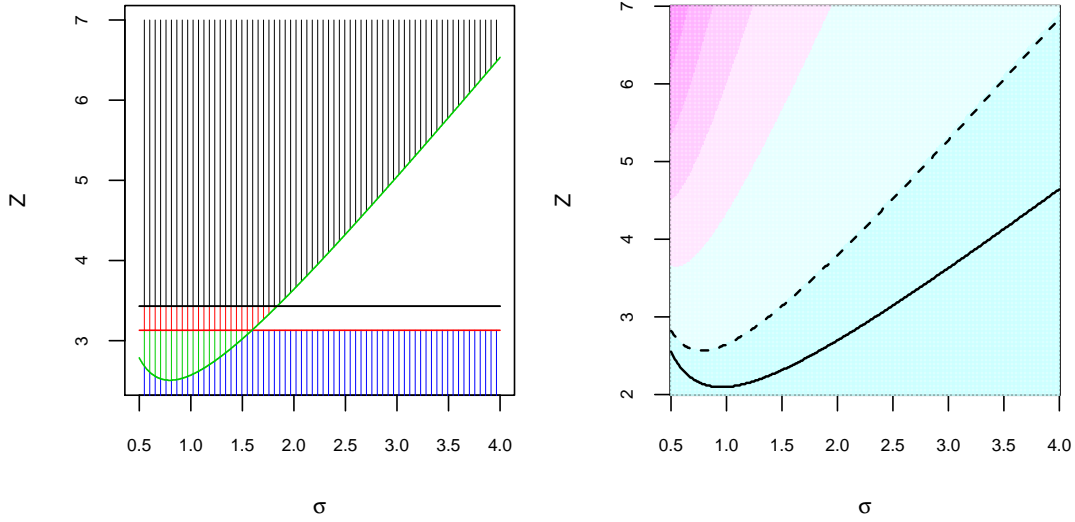


Figure 1: Left: Rejection regions for the p -value approach (black line), z -value approach (red line) and full data approach (green line) as a function of Z and σ . Approaches reject for all points above their corresponding line. Right: Heat map of relative proportions (on log scale) of alternative vs null hypotheses for different Z and σ . Blue corresponds to lower ratios and purple to higher ratios. The solid black line represents equal fractions of null and alternative, while the dashed line corresponds to three times as many alternative as null.

Section A of the Appendix. For the model given by (2.8) these rules correspond to:

$$\begin{aligned}\delta^p &= \{\mathbb{I}(P_i \leq 0.0006) : 1 \leq i \leq m\} = \{\mathbb{I}(|Z_i| \geq 3.43) : 1 \leq i \leq m\}, \\ \delta^z &= \{\mathbb{I}(\mathbb{P}(H_0|Z_i) \leq 0.24) : 1 \leq i \leq m\} = \{\mathbb{I}(Z_i \geq 3.13) : 1 \leq i \leq m\}, \\ \delta^{\text{full}} &= \{\mathbb{I}(\mathbb{P}(H_0|X_i, \sigma_i) \leq 0.28) : 1 \leq i \leq m\},\end{aligned}$$

with the thresholds chosen such that the FDR is exactly 10% for all three approaches. However, while the FDRs of these three methods are identical, the average powers, $\text{AP}(\delta) = \frac{1}{m\pi} \mathbb{E}(\sum_{i=1}^m \theta_i \delta_i)$, differ significantly:

$$\text{AP}(\delta^p) = 5.0\%, \quad \text{AP}(\delta^z) = 7.2\%, \quad \text{AP}(\delta^{\text{full}}) = 10.5\%. \quad (2.9)$$

To better understand these differences consider the left hand plot in Figure 1, which illustrates the rejection regions for each approach as a function of Z and σ^2 . In the blue

²The p -value method will also reject for large negative values of Z but, to keep the figure readable, we have not plotted that region.

region all methods fail to reject the null hypothesis, while all methods reject in the black region. The green region corresponds to the space where the full data approach rejects the null while the other two methods do not. Alternatively, in the red region both the z -value and full data methods reject while the p -value approach fails to do so. Finally, in the white region the full data approach fails to reject while the z -value method does reject.

We first compare δ^z and δ^p . Let π^+ and π^- denote the proportions of positive effects and negative effects, respectively. Then $\pi^+ = 0.1$ and $\pi^- = 0$. This asymmetry of the alternative distribution can be captured by δ^z , which uses a one-sided rejection region. (Note that this asymmetric rejection region is not pre-specified but a consequence of theoretical derivation. In practice δ^z can be emulated by an adaptive z -value approach that is fully data-driven (Sun and Cai, 2007).) By contrast, δ^p enforces a two-sided rejection region that is symmetrical about 0, trading off extra rejections in the region $Z_i \leq -3.43$ for fewer rejections in the region where $3.13 \leq Z_i \leq 3.43$. As all nonzero effects are positive, negative z -values are highly unlikely to come from the alternative; this accounts for the 2.2% loss in AP for the p -value method. Next consider δ^{full} vs δ^z . The full data approach trades off extra rejections in the green space for fewer rejections in the white space. This may seem like a sub-optimal trade-off given that the green space is smaller. However, the green space actually contains many more true alternative hypotheses. Approximately 3.8% of the true alternatives occur in the green region as opposed to only 0.5% in the white region, which accounts for the 3.3% higher AP for the full data approach.

At first Figure 1 may appear counterintuitive. Why should we reject for low z -values in the green region but fail to reject for high z -values in the white region? The key observation here is that *not all z -values are created equal*. In the green region the observed data is far more consistent with the alternative hypothesis than the null hypothesis. For example, with $Z = 4$ and $\sigma = 0.5$ our observed X is four standard deviations from the null mean but exactly equal to the alternative mean. Alternatively, while it is true that in the white region the high z -values suggest that the data are inconsistent with the null hypothesis, *they are also highly inconsistent with the alternative hypothesis*. For example, with $Z = 4$ and $\sigma = 2$ our observed X is 8, which is four standard deviations from the null mean, but also three standard deviations from the alternative mean. Given that 90% of observations come from the null hypothesis, we do not have conclusive evidence as to whether this data

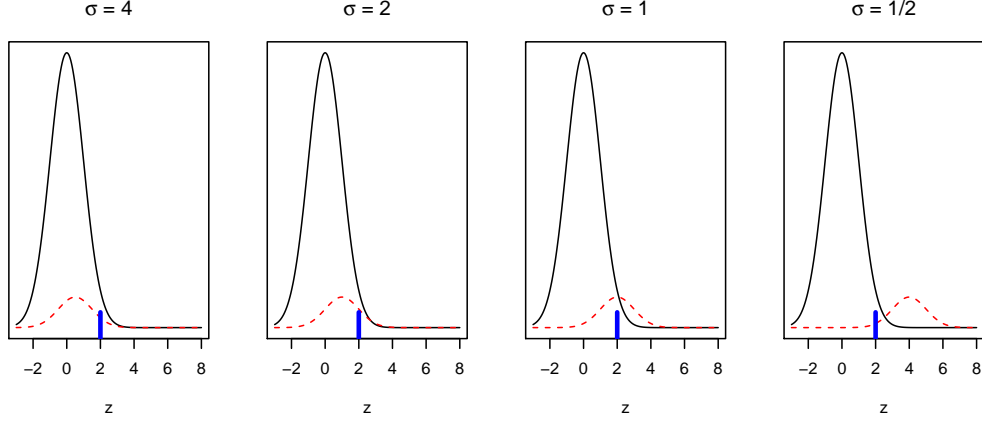


Figure 2: Plots of the density functions of Z under the null hypothesis (black solid) and alternative hypothesis (red dashed) for different values of σ . The blue line represents an observation at $Z = 2$.

is from the null or alternative. A z -value of 4 with $\sigma = 0.5$ is far more likely to come from the alternative hypothesis than is a z -value of 4 with $\sigma = 2$.

The right hand plot of Figure 1 makes this clear. Here we have plotted (on a log scale) the relative proportions of alternative vs null hypotheses for different Z and σ . Blue corresponds to lower ratios and purple to higher ratios. The solid black line represents equal fractions of null and alternative, while the dashed line corresponds to three times as many alternative as null. Clearly, for the same z -value, alternative hypotheses are relatively more common for low σ values. Notice how closely the shape of the dashed line maps the green rejection boundary in the left hand plot, which indicates that the full data method is correctly capturing the regions with most alternative hypotheses. By contrast, the p -value and z -value methods fail to correctly adjust for different values of σ .

Figure 2 provides one further way to understand the effect of standardizing the data. Here we have plotted the density functions of Z under the null hypothesis (black solid) and alternative hypothesis (red dashed) for different values of σ . The densities have been multiplied by the relative probability of each hypothesis occurring so points where the densities cross correspond to an equal likelihood for either hypothesis. The blue line represents an observation, which is fixed at $Z = 2$ in each plot. The alternative density is centered at $Z = 2/\sigma$ so when σ is large the standardized null and alternative are very similar, making

it hard to know which distribution $Z = 2$ belongs to. As σ decreases the standardized alternative distribution moves away from the null and becomes more consistent with $Z = 2$. However, eventually the alternative moves past $Z = 2$ and it again becomes unclear which distribution our data belongs to. Standardizing means that the null hypothesis is consistent for all values of σ but the alternative hypothesis can change dramatically as a function of the standard deviation.

To summarize, the information loss occurred in both steps of data processing (2.7) reveals *the essential role of the alternative distribution* in simultaneous testing. This structure of the alternative is not captured by the p -value, which is calculated only based on the null. Our result (2.9) in the toy example shows that by exploiting (i) the overall asymmetry of the alternative via the z -value and (ii) the heterogeneity among individual alternatives via the full data, the average power of conventional p -value based methods can be doubled.

2.3 Heteroscedasticity and empirical null distribution

In the context of simultaneous testing with composite null hypotheses, Sun and McLain (2012) argued that the conventional testing framework, which involves rescaling or standardization, can become problematic:

“In multiple testing problems where the null is simple ($H_{0,i} : \mu_i = 0$), the heteroscedasticity in errors can be removed by rescaling all σ_i to 1. However, when the null is composite, such a rescaling step would distort the scientific question.”

Sun and McLain (2012) further proposed the concept of *empirical composite null* as an extension of Efron’s *empirical null* (Efron, 2004b) for testing composite nulls $H_{0,i} : \mu_i \in [-a_0, a_0]$ under heteroscedastic models. It is important to note that the main message of this article, which focuses on the impact of heteroscedasticity on the alternative instead of the null, is fundamentally different from that in Sun and McLain (2012). In fact, we show that even when the null is simple, the heteroscedasticity still matters. Our finding, which somehow contradicts the above quotes, is more striking and even counter-intuitive. Moreover, we shall see that our data-driven HART procedure, which is based on Tweedie’s formula (or the f -modeling approach, Efron, 2011), is very different from the deconvoluting

kernel method (or g -modeling approach) in Sun and McLain (2012)³. The new two-step bivariate estimator in Section 3.2 is novel and highly nontrivial; the techniques employed in the proofs of theory are also very different.

3 HART: Heteroscedasticity Adjusted Ranking and Thresholding

The example in the previous section presents a setting where hypothesis tests based on the full data (X_i, σ_i) can produce higher power than that from using the standardized data Z_i . In this section we formalize this idea and show that the result holds in general for heteroscedasticity problems. We first assume that the distributional information is known and derive an oracle rule based on full data in Section 3.1. Section 3.2 develops data-driven schemes and computational algorithms to implement the oracle rule. Finally theoretical properties of the proposed method are established in Section 3.3.

3.1 The oracle rule under heteroscedasticity

Note that the models given by (2.1) and (2.2) imply that

$$X_i | \sigma_i \stackrel{ind}{\sim} f_{\sigma_i}(x) = (1 - \pi)f_{0,\sigma_i}(x) + \pi f_{1,\sigma_i}(x), \quad (3.1)$$

where $f_{0,\sigma}(x) = \frac{1}{\sigma}\phi(x/\sigma)$ is the null density, $f_{1,\sigma}(x) = \frac{1}{\sigma} \int \phi_\sigma\left(\frac{x-\mu}{\sigma}\right) g_\mu(\mu) d\mu$ is the alternative density, $\phi(x)$ is the density of a standard normal variable, and $f_\sigma(x)$ is the mixture density. For standardized data $Z_i = X_i/\sigma_i$, Model 3.1 reduces to

$$Z_i \stackrel{iid}{\sim} f(z) = (1 - \pi)f_0(z) + \pi f_1(z), \quad (3.2)$$

where $f_0(z) = \phi(z)$, $f_1(z)$ is the non-null density, and $f(z)$ is the mixture density of the z -values. As discussed previously, a standard approach involves converting the z -value to

³ The deconvoluting kernel method has an extremely slow convergence rate. Our numerical studies show that the method in Sun and McLain (2012) only works for composite nulls where the uncertainties in estimation can be smoothed out over an interval $[-a_0, a_0]$. However, the deconvoluting method is highly unstable and does not work well when testing simple nulls $H_{0,i} : \mu_i = 0$. Our numerical results show that the two-step method in Section 3.2 works much better.

a two-sided p -value $P_i = 2\Phi(-|Z_i|)$, where $\Phi(\cdot)$ is the standard normal cdf. The mixture model based on p -values is

$$P_i \stackrel{iid}{\sim} g(p) = (1 - \pi)\mathbb{I}_{[0,1]}(p) + \pi g_1(p), \quad \text{for } p \in [0, 1], \quad (3.3)$$

where $\mathbb{I}(\cdot)$ is an indicator function, and $g(\cdot)$ and $g_1(\cdot)$ are the mixture density and non-null density of the p -values, respectively. Models 3.2 and 3.3 provide a powerful and flexible framework for large-scale inference and have been used in a range of related problems such as signal detection, sparsity estimation and multiple testing [e.g. Efron et al. (2001); Storey (2002); Genovese and Wasserman (2002); Donoho and Jin (2004); Newton et al. (2004); Jin and Cai (2007)].

The oracle FDR procedure for Models 3.2 and 3.3 are both known. We first review the oracle z -value procedure (Sun and Cai, 2007). Define the local FDR (Efron et al., 2001)

$$\text{Lfdr}_i = \mathbb{P}(H_0|z_i) = \mathbb{P}(\theta_i = 0|z_i) = \frac{(1 - \pi)f_0(z_i)}{f(z_i)}. \quad (3.4)$$

Then Sun and Cai (2007) showed that the optimal z -value FDR procedure is given by

$$\boldsymbol{\delta}^z = [\mathbb{I}\{\text{Lfdr}(z_i) < c^*\} : 1 \leq i \leq m], \quad (3.5)$$

where c^* is the largest Lfdr threshold such that $\text{mFDR} \leq \alpha$. Similarly, Genovese and Wasserman (2002) showed that the optimal p -value based FDR procedure is given by

$$\boldsymbol{\delta}^p = [\mathbb{I}\{P_i < c^*\} : 1 \leq i \leq m], \quad (3.6)$$

where c^* is the largest p -value threshold such that $\text{mFDR} \leq \alpha$.

Next we derive the oracle rule based on m pairs $\{(x_i, \sigma_i) : i = 1, \dots, m\}$. This new problem can be recast and solved in the framework of multiple testing with a covariate sequence. Consider Model 3.1 and define the heterogeneity-adjusted significance index

$$T_i \equiv T(x_i, \sigma_i) = \mathbb{P}(\theta_i = 0|x_i, \sigma_i) = \frac{(1 - \pi)f_{0, \sigma_i}(x_i)}{f_{\sigma_i}(x_i)}. \quad (3.7)$$

Let $Q(t)$ denote the mFDR level of the testing rule $[\mathbb{I}\{T_i < t\} : 1 \leq i \leq m]$. Then the oracle

full data procedure is denoted

$$\boldsymbol{\delta}^{\text{full}} = [\mathbb{I}\{T_i < t^*\} : 1 \leq i \leq m], \quad (3.8)$$

where $t^* = \sup\{t : Q(t) \leq \alpha\}$.

The next theorem provides the key result showing that $\boldsymbol{\delta}^{\text{full}}$ has highest power amongst all α -level FDR rules based on $\{(x_i, \sigma_i) : i = 1, \dots, m\}$.

Theorem 1 *Let \mathcal{D}_α be the collection of all testing rules based on $\{(x_i, \sigma_i) : i = 1, \dots, m\}$ such that $m\text{FDR}_\delta \leq \alpha$. Then $\text{ETP}_\delta \leq \text{ETP}_{\delta^{\text{full}}}$ for any $\delta \in \mathcal{D}_\alpha$. In particular we have*

$$\text{ETP}_{\delta^p} \leq \text{ETP}_{\delta^z} \leq \text{ETP}_{\delta^{\text{full}}}.$$

Based on Theorem 1, our proposed methodology employs a *heteroscedasticity-adjusted ranking and thresholding* (HART) rule that operates in two steps: first rank all hypotheses according to T_i and then reject all hypotheses with $T_i \leq t^*$. We discuss in Section 3.2 our finite sample approach for implementing HART using estimates for T_i and t^* .

3.2 Data-driven procedure and computational algorithms

We first discuss how to estimate T_i and then turn to t^* . Inspecting T_i 's formula (3.7), the null density $f_{0,\sigma_i}(x_i)$ is known and the non-null proportion π can be estimated by $\hat{\pi}$ using existing methods such as Storey's estimator (Storey, 2002) or Jin-Cai's estimator (Jin and Cai, 2007). Hence we focus on the problem of estimating $f_{\sigma_i}(x_i)$.

There are two possible approaches for implementing this step. The first involves directly estimating $f_{\sigma_i}(x_i)$ while the second is implemented by first estimating $f_{1,\sigma_i}(x_i)$ and then computing the marginal distribution via

$$\hat{f}_{\sigma_i}(x_i) = (1 - \hat{\pi})f_{0,\sigma_i}(x_i) + \hat{\pi}\hat{f}_{1,\sigma_i}(x_i). \quad (3.9)$$

Our theoretical and empirical results strongly suggest that this latter approach provides superior results so we adopt this method.

Remark 1 The main concern about the direct estimation of $f_{\sigma_i}(x_i)$ is that the tail areas

of the mixture density are of the greatest interest in multiple testing but unfortunately the hardest parts to accurately estimate due to the few observations in the tails. The fact that $f_{\sigma_i}(x_i)$ appears in the denominator exacerbates the situation. The decomposition in (3.9) increases the stability of the density by incorporating a known part of null density.

Standard bivariate kernel methods (Silverman, 1986; Wand and Jones, 1994) are not suitable for estimating $f_{1,\sigma_i}(x_i)$ because, unlike a typical variable, σ_i plays a special role in a density function and needs to be modeled carefully. Fu et al. (2018) recently addressed a closely related problem using the following weighted bivariate kernel estimator:

$$\hat{f}_{\sigma}^*(x) := \sum_{j=1}^m \frac{\phi_{h_{\sigma}}(\sigma - \sigma_j)}{\sum_{j=1}^m \phi_{h_{\sigma}}(\sigma - \sigma_j)} \phi_{h_{xj}}(x - x_j), \quad (3.10)$$

where $\mathbf{h} = (h_x, h_{\sigma})$ is a pair of bandwidths, $\phi_{h_{\sigma}}(\sigma - \sigma_j) / \{\sum_{j=1}^m \phi_{h_{\sigma}}(\sigma - \sigma_j)\}$ determines the contribution of (x_j, σ_j) based on σ_j , $h_{xj} = h_x \sigma_j$ is a bandwidth that varies across j , and $\phi_h(z) = \frac{1}{\sqrt{2\pi}h} \exp\left\{-\frac{z^2}{2h^2}\right\}$ is a Gaussian kernel. The variable bandwidth h_{xj} up-weights/down-weights observations corresponding to small/large σ_j ; this suitably adjusts for the heteroscedasticity in the data.

Let $\mathcal{M}_1 = \{i : \theta_i = 1\}$. In the ideal setting where θ_j is observed one could extend (3.10) to estimate $f_{1,\sigma_i}(x_i)$ via

$$\tilde{f}_{1,\sigma}(x) = \sum_{j \in \mathcal{M}_1} \frac{\phi_{h_{\sigma}}(\sigma - \sigma_j)}{\sum_{k \in \mathcal{M}_1} \phi_{h_{\sigma}}(\sigma - \sigma_k)} \phi_{h_{xj}}(x - x_j). \quad (3.11)$$

Given that θ_j is unknown, we cannot directly implement (3.11). Instead we apply a weighted version of (3.11),

$$\hat{f}_{1,\sigma_i}(x_i) = \sum_{j=1}^m \frac{\hat{w}_j \phi_{h_{\sigma}}(\sigma_i - \sigma_j)}{\sum_{k=1}^m \hat{w}_k \phi_{h_{\sigma}}(\sigma_i - \sigma_k)} \phi_{h_{xj}}(x_i - x_j) \quad (3.12)$$

with weights \hat{w}_j equal to an estimate of $P(\theta_j = 1 | x_j, \sigma_j)$. In particular we adopt a two step approach:

1. Compute $\hat{f}_{1,\sigma_i}^{(0)}(x_i)$ via (3.12) with initial weights $\hat{w}_j^{(0)} = (1 - \hat{T}_j^{(0)})$ for all j , where $\hat{T}_j^{(0)} = \min\left\{\frac{(1-\hat{\pi})f_{0,\sigma_j}(x_j)}{\hat{f}_{\sigma_j}^*(x_j)}, 1\right\}$, $\hat{\pi}$ is the estimated non-null proportion, and $\hat{f}_{\sigma_j}^*(x_j)$ is computed using (3.10).

2. Compute $\hat{f}_{1,\sigma_i}^{(1)}(x_i)$ via (3.12) with updated weights $\hat{w}_j^{(1)} = (1 - \hat{T}_j^{(1)})$ where

$$\hat{T}_j^{(1)} = \frac{(1 - \hat{\pi})f_{0,\sigma_j}(x_j)}{(1 - \hat{\pi})f_{0,\sigma_j}(x_j) + \hat{\pi}\hat{f}_{1,\sigma_j}^{(0)}(x_j)}.$$

This leads to our final estimate for $T_i = \mathbb{P}(H_0|x_i, \sigma_i)$:

$$\hat{T}_i = \hat{T}_i^{(2)} = \frac{(1 - \hat{\pi})f_{0,\sigma_i}(x_i)}{(1 - \hat{\pi})f_{0,\sigma_i}(x_i) + \hat{\pi}\hat{f}_{1,\sigma_i}^{(1)}(x_i)}.$$

In the next section, we carry out a detailed theoretical analysis to show that both $\hat{f}_{\sigma_i}(x_i)$ and \hat{T}_i are consistent estimators with $\mathbb{E}\|\hat{f}_{\sigma_i} - f_{\sigma_i}\|^2 = \mathbb{E} \int \{\hat{f}_{\sigma_i}(x) - f_{\sigma_i}(x)\}^2 dx \rightarrow 0$ and $\hat{T}_i \xrightarrow{P} T_i$, uniformly for all i .

To implement the oracle rule (3.8), we need to estimate the optimal threshold t^* , which can be found by carrying out the following simple stepwise procedure.

Procedure 1 (data-driven HART procedure) *Rank hypotheses by increasing order of \hat{T}_i . Denote the sorted ranking statistics $\hat{T}_{(1)} \leq \dots \leq \hat{T}_{(m)}$ and $H_{(1)}, \dots, H_{(m)}$ the corresponding hypotheses. Let*

$$k = \max \left\{ j : \frac{1}{j} \sum_{i=1}^j \hat{T}_{(i)} \leq \alpha \right\}.$$

Then reject the corresponding ordered hypotheses, $H_{(1)}, \dots, H_{(k)}$.

The idea of the above procedure is that if the first j hypotheses are rejected, then the moving average $\frac{1}{j} \sum_{i=1}^j \hat{T}_{(i)}$ provides a good estimate of the false discovery proportion, which is required to fulfill the FDR constraint. Comparing with the oracle rule (3.8), Procedure 1 can be viewed as its plug-in version:

$$\boldsymbol{\delta}^{dd} = \{\mathbb{I}(\hat{T}_i \leq \hat{t}^*) : 1 \leq i \leq m\}, \text{ where } \hat{t}^* = \hat{T}_{(k)}. \quad (3.13)$$

The theoretical properties of Procedure 1 are studied in the next section.

3.3 Theoretical properties of HART

In Section 3.1, we have shown that the (full data) oracle rule $\boldsymbol{\delta}^{\text{full}}$ (3.8) is valid and optimal for FDR analysis. This section discusses the key theoretical result, Theorem 2, which shows

that the performance of $\boldsymbol{\delta}^{\text{full}}$ can be achieved by its finite sample version $\boldsymbol{\delta}^{\text{dd}}$ (3.13) when $m \rightarrow \infty$. Inspecting (3.13), the main steps involve showing that both \hat{T}_i and \hat{t}^* are “close” to their oracle counterparts. To ensure good performance of the proposed procedure, we require the following conditions.

(C1) $\text{supp}(g_\sigma) \in (M_1, M_2)$ and $\text{supp}(g_\mu) \in (-M, M)$ for some $M_1 > 0$, $M_2 < \infty$, $M < \infty$.

(C2) $h_x = o\{(\log m)^{-1}\}$ and $\lim_{m \rightarrow \infty} mh_x = \infty$.

(C3) $\lim_{m \rightarrow \infty} m^{1-\delta} h_\sigma h_x^2 = \infty$ and $\lim_{m \rightarrow \infty} m^{-\delta/2} h_\sigma^2 h_x^{-1} \rightarrow 0$ for some $\delta > 0$.

(C4) $\hat{\pi} \xrightarrow{P} \pi$.

Remark 2 Condition (C2) is standard in density estimation theory, see for example Brown and Greenshtein (2009) and Silverman (1986). Condition (C3) is satisfied for most popular choices of h_x , for example in Wand and Jones (1994), where $h_x \sim m^{-1/5}$ minimizes mean integrated squared error (MISE). Jin-Cai’s estimator Jin and Cai (2007) fulfills Condition (C4) in a wide class of mixture models.

Our theory is divided into two parts. The next proposition establishes the theoretical properties of the proposed density estimator \hat{f}_σ and the plug-in statistic \hat{T}_i . The convergence of \hat{t}^* to t^* and the asymptotic properties of $\boldsymbol{\delta}^{\text{dd}}$ are established in Theorem 2.

Proposition 1 *Suppose Conditions (C1) to (C5) hold. Then*

$$\mathbb{E} \|\hat{f}_\sigma - f_\sigma\|^2 = \mathbb{E} \int \{\hat{f}_\sigma(x) - f_\sigma(x)\}^2 dx \rightarrow 0,$$

where the expectation \mathbb{E} is taken over $(\mathbf{X}, \boldsymbol{\sigma}, \boldsymbol{\mu})$. Further, we have $\hat{T}_i \xrightarrow{P} T_i$.

Next we turn to the performance of our data-driven procedure $\boldsymbol{\delta}^{\text{dd}}$ when $m \rightarrow \infty$. A key step in the theoretical development is to show that $\hat{t}^* \xrightarrow{P} t^*$, where \hat{t}^* and t^* are defined in (3.13) and (3.8), respectively.

Theorem 2 *Under the conditions in Proposition 1, we have $\hat{t}^* \xrightarrow{P} t^*$. Further, both the $m\text{FDR}$ and FDR of $\boldsymbol{\delta}^{\text{dd}}$ are controlled at level $\alpha + o(1)$, and $\text{ETP}_{\boldsymbol{\delta}^{\text{dd}}} / \text{ETP}_{\boldsymbol{\delta}^{\text{full}}} = 1 + o(1)$.*

In combination with Theorem 1, these results demonstrate that the proposed finite sample HART procedure (Procedure 1) is asymptotically valid and optimal.

4 Simulation

We first describe the implementation of HART in Section 4.1. Section 4.2 presents results for the general setting where σ_i comes from a continuous density function. In Section 4.3, we further investigate the effect of heterogeneity under a mixture model where σ_i takes on one of two distinct values.

4.1 Implementation of HART

The accurate estimation of \hat{T}_i is crucial for ensuring good performance of the HART procedure. The key quantity is the bivariate kernel density estimator $\hat{f}_{1,\sigma}(x)$, which depends on the choice of tuning parameters $\mathbf{h} = (h_x, h_\sigma)$. Note that the ranking and selection process in Procedure 1 only involves small \hat{T}_i . To improve accuracy, the bandwidth should be chosen based on the pairs (x_i, σ_i) that are less likely to come from the null. We first implement Jin and Cai’s method (Jin and Cai, 2007) to estimate the overall proportion of non-nulls in the data, denoted $\hat{\pi}$. We then compute h_x and h_σ by applying Silverman’s rule of thumb (Silverman, 1986) to the subset of the observations $\{x_i : P_i < \hat{\pi}\}$. When implementing HART, a jackknifed method is recommended. Specifically, we first estimate $f_\sigma(x)$ using the data without (X_i, S_i) , and then plug-in the unused data (X_i, S_i) to calculate \hat{T}_i . This jackknifed method can increase the stability of the density estimator. As shown in the proof of Proposition 1, the asymptotic properties of \hat{T}_i hold for both the regular and jackknifed approaches.

4.2 Comparison in general settings

We consider simulation settings according to Models 2.1 and 2.2, where σ_i are uniformly generated from $U[1, \sigma_{max}]$. We then generate X_i from a two-component normal mixture model

$$X_i | \sigma_i \stackrel{iid}{\sim} (1 - \pi)N(0, \sigma_i^2) + \pi N(2, \sigma_i^2).$$

In the first setting, we fix $\sigma_{max} = 3$ and vary π from 0.05 to 0.15. In the second setting, we fix $\pi = 0.1$ and vary σ_{max} from 2.5 to 3.5. Four methods are compared: the ideal full data oracle procedure (OR), the z -value oracle procedure of Sun and Cai (2007) (ZOR), the Benjamini-Hochberg procedure (BH) and the proposed data-driven HART procedure

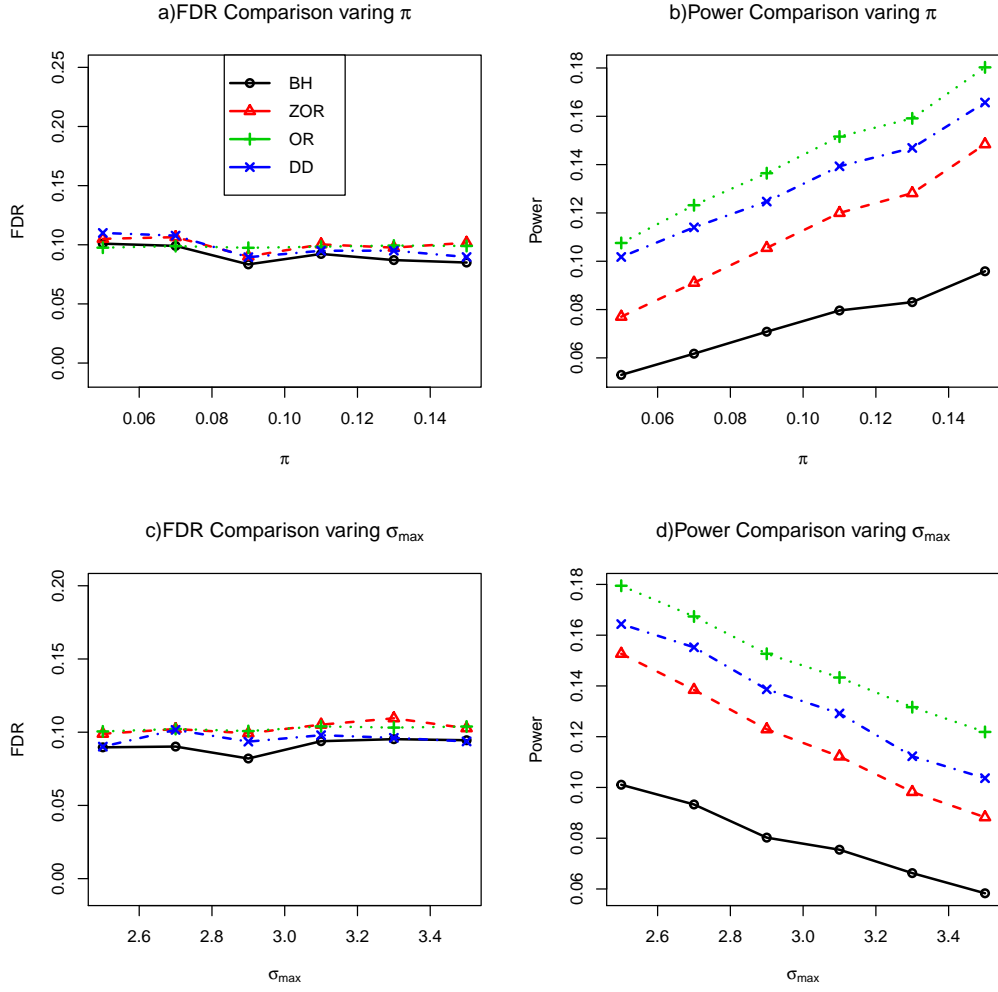


Figure 3: Comparison when σ_i is generated from a uniform distribution. We vary π in the top row and σ_{\max} in the bottom row. All methods control the FDR at the nominal level. DD has roughly the same FDR but higher power compared to ZOR in all settings.

(DD). The nominal FDR level is set to $\alpha = 0.1$. For each setting, the number of tests is $m = 20,000$. Each simulation is also run over 100 repetitions. Then, the FDR is estimated as the average of the false discovery proportion $\text{FDP}(\delta) = \sum_{i=1}^m \{(1 - \theta_i)\delta_i\} / (\sum_{i=1}^m \delta_i \vee 1)$ and the average power is estimated as the average proportion of true positives that are correctly identified, $\sum_{i=1}^m (\theta_i \delta_i) / (mp)$, both over the number of repetitions. The results for differing values of π and σ_{\max} are respectively displayed in the first and second rows of Figure 3.

Next we discuss some important patterns of the plots and provide interpretations. Panel

(a) of Figure 3 shows that all methods appropriately control FDR at the nominal level, with BH being slightly conservative. Panel (b) illustrates the advantage of the proposed HART procedure over existing methods. When π is small, the power of OR can be 40% higher than ZOR. This shows that exploiting the structural information of the variance can be extremely beneficial. DD has lower power compared to OR due to the inaccuracy in estimation. However, DD still dominates ZOR and BH in all settings. We can also see that ZOR dominates BH and the efficiency gain increases as π increases. To explain the power gain of ZOR over BH, let π^+ and π^- denote the proportion of true positive signals and true negative signals, respectively. Then $\pi^+ = \pi$ and $\pi^- = 0$. This asymmetry can be captured by ZOR, which uses a one-sided rejection region. By contrast, BH adopts a two-sided symmetric rejection region. Under the setting being considered, the power loss due to the conservativeness of BH is essentially negligible, whereas the failure of capturing important structural information in the alternative accounts for most power loss. From the second row of Figure 3, we can again see that all methods control the FDR at the nominal level. OR dominates the other three methods in all settings. DD is less powerful than OR but has a clear advantage over ZOR with slightly lower FDR and higher power.

4.3 Comparison under a two-group model

To illustrate the heteroscedasticity effect more clearly, we conduct a simulation using a simpler model where σ_i takes on one of two distinct values. The goal is to illustrate that the heterogeneity adjustment is more useful when there is greater variation in the standard deviations among the testing units.

Consider the setup in Models 2.1 and 2.2. We first draw σ_i randomly from two possible values $\{\sigma_a, \sigma_b\}$ with equal probability, and then generate X_i from a two-point normal mixture model $X_i|\sigma_i \stackrel{iid}{\sim} (1 - \pi)N(0, \sigma_i^2) + \pi N(\mu, \sigma_i^2)$. In this simpler setting, it is easy to show that HART reduces to the CLfdr method in Cai and Sun (2009), where the conditional Lfdr statistics are calculated for separate groups defined by σ_a and σ_b . As previously, we apply BH, ZOR, OR and DD to data with $m = 20,000$ tests and the experiment repeated on 100 data sets. We fix $\pi = 0.1$, $\mu = 2.5$, $\sigma_a = 1$ and vary σ_b from 1.5 to 3. The FDRs and powers of different methods are plotted as functions of σ_b , with results summarized in the first row of Figure 4. In the second row, we plot the group-wise z -value cutoffs and

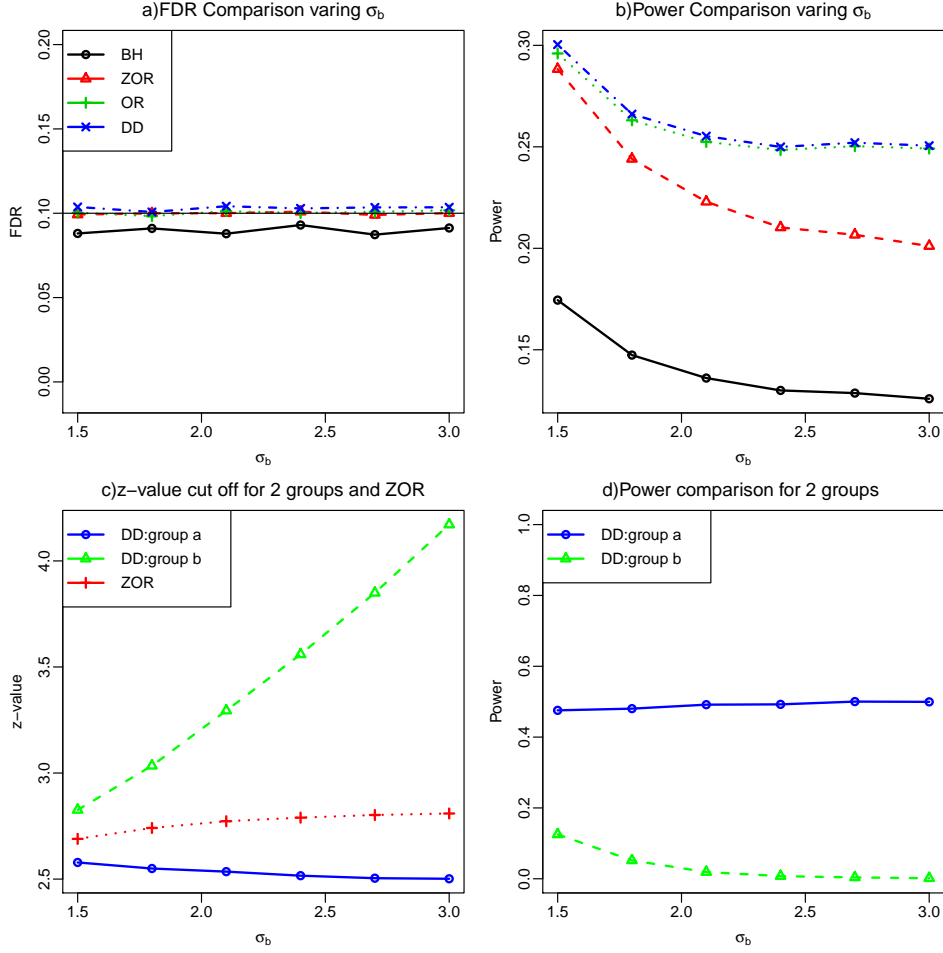


Figure 4: Two groups with varying σ_b from 1.5 to 3. As σ_b increases, the cut-off for group a decreases whereas the cut-off for group b increases. The power for tests in group b drops quickly as σ_b increases. This corroborates our calculations in the toy example in Section 2.2 and the patterns revealed by Figure 1.

group-wise powers as functions of σ_b for the DD method.

We can see that DD has almost identical performance to OR, and the power gain over ZOR becomes more pronounced as σ_b increases. This is intuitive, because more variation in σ tends to lead to more information loss in standardization. The bottom row shows the z -value cutoffs for ZOR and DD for each group. We can see that in comparison to ZOR, which uses a single z -value cutoff, HART uses different cutoffs for each group. The z -value cutoff is bigger for the group with larger variance, and the gap between the two cutoffs increases as the degree of heterogeneity increases. In Panel d), we can see that the

power of Group b decreases as σ_b increases. These interesting patterns corroborate those we observed in our toy example in Section 2.2.

5 Data Analysis

This section compares the adaptive z -value procedure (AZ, the data-driven implementation of ZOR, Sun and Cai (2007)), BH, and HART on a microarray data set. The data set measures expression levels of 12,625 genes for patients with multiple myeloma, 36 for whom magnetic resonance imaging (MRI) detected focal lesions of bone (lesions), and 137 for whom MRI scans could not detect focal lesions (without lesions) of bone (Tian et al., 2003). For each gene, we calculate the differential gene expression levels (X_i) and standard errors (S_i). The FDR level is set at $\alpha = 0.1$.

We first address two important practical issues. The first issue is that the theoretical null $N(0, 1)$ (red curve on the left panel of Figure 5) is much narrower compared to the histogram of z -values. Efron (2004a) argued that a seemingly small deviation from the theoretical z -curve can lead to severely distorted FDR analysis. For this data set, the analysis based on the theoretical null would inappropriately reject too many hypotheses, resulting in a very high FDR. To address the distortion of the null, we adopted the *empirical null* approach (Efron, 2004a) in our analysis. Specifically, we first used the middle part of the histogram, which contains 99% of the data, to estimate the null distribution as $N(0, 1.30^2)$ [see Efron (2004a) for more details]. The new p -values are then converted from the z -values based on the estimated empirical null: $P_i^* = 2\Phi^*(-2|Z_i|)$, where Φ^* is the CDF of a $N(0, 1.30^2)$ variable. We can see from Figure 5 that the empirical null (green curve) provides a better fit to the histogram of z -values. Another evidence for the suitability of the empirical null approach is that the histogram of the estimated p -values looks closer to uniform compared to that of original p -values. The uniformity assumption is crucial for ensuring the validity of p -value based procedures.

The second issue is the estimation of $f_\sigma(x)$, which usually requires a relatively large sample size to ensure good precision. Figure 6 presents the histogram of S_i and scatter plot of S_i vs Z_i . Based on the histogram, we propose to only focus on data points with S_i less than 1 (12172 out of 12625 genes are kept in the analysis) to ensure the estimation

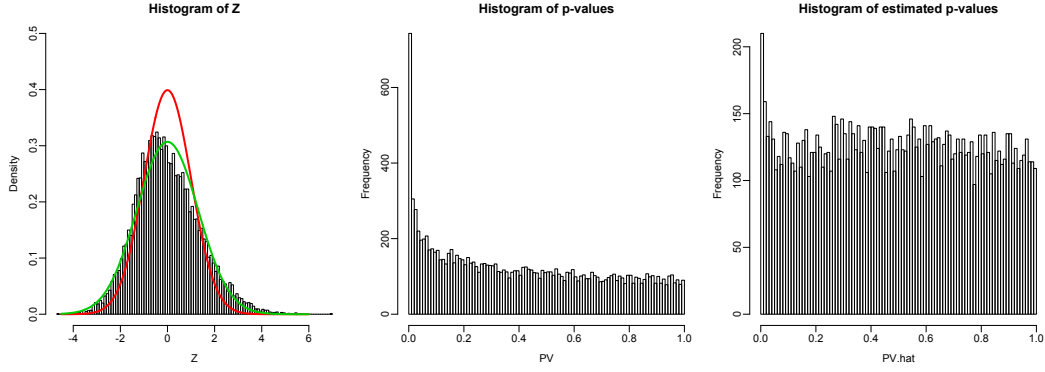


Figure 5: Left: histogram of z -values: the estimated empirical null $N(0, 1.3^2)$ (green line) seems to provide a better fit to the data compared to the theoretical null $N(0, 1)$ (red line). Middle: histogram of original p -values. Right: histogram of estimated p -values based on the empirical null. The z -value histogram suggests that the theoretical null is inappropriate (too narrow, leading to too many rejections). The use of an empirical null corrects the non-uniformity of the histogram of the p -values.

accuracy of \hat{T}_i . Compared to conventional approaches, there is no efficiency loss because no hypothesis with $S_i > 1$ is rejected by BH at $\alpha = 0.1$ – note that the BH p -value cutoff is 6×10^{-5} , which corresponds to a z -value cutoff of 5.22; see also Figure 7. (If BH rejects hypotheses with large S_i , we recommend to carry out a group-wise FDR analysis, which first tests hypotheses at α in separate groups and then combines the testing results, as suggested by Efron (2008a).)

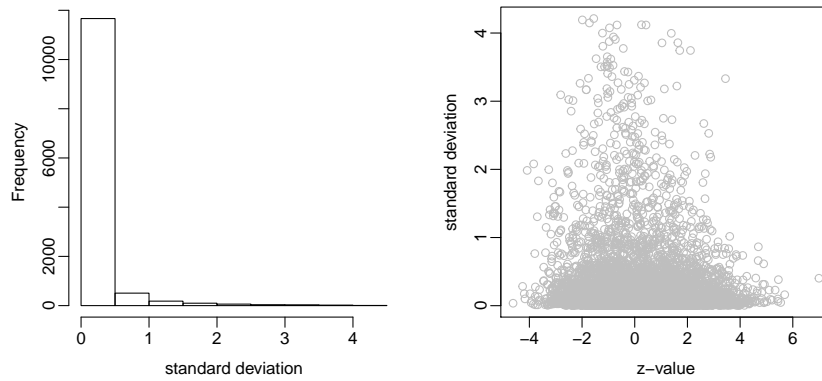


Figure 6: Histogram of S_i (left), scatter plot of (Z_i, S_i) (right)

Finally we apply BH, AZ and HART to the data points with $S_i < 1$. BH uses the new p -

Table 1: Numbers of genes (% of total) that are selected by each method.

α -level	BH	AZ	HART
0.1	8 (0.07%)	25 (0.2%)	122 (1%)

values P_i^* based on the estimated empirical null $N(0, 1.3^2)$. Similarly AZ uses Lfdr statistics where the null is taken as the density of a $N(0, 1.3^2)$ variable. When implementing HART, we estimate the non-null proportion π using Jin-Cai’s method with the empirical null taken as $N(0, 1.3^2)$. We further employ the jackknifed method to estimate $f_\sigma(x)$ by following the steps in Section 4.1. We summarize the number of rejections by each method in Table 1 and display the testing results in Figure 7, where we have marked rejected hypotheses by each method using different colors.

HART rejects more hypotheses than BH and AZ. The numbers should be interpreted with caution as BH and AZ have employed the empirical null $N(0, 1.3^2)$ whereas HART has utilized null density $N(0, \sigma_i^2)$ conditioned on individual σ_i – it remains an open issue how to extend the empirical null approach to the heteroscedastic case. Since we do not know the ground truth, it is difficult to assess the power gains. However, the key point of this analysis, and the focus of our paper, is to compare the *shapes of rejection regions* to gain some insights on the differences between the methods. It can be seen that for this data set, the rejection rules of BH and AZ only depend on Z_i . By contrast, the rejection region for HART depends on both Z_i and S_i . HART rejects more z -values when S_i is small compared to BH and AZ. Moreover, HART does not reject any hypothesis when S_i is large. This pattern is consistent with the intuitions we gleaned from the illustrative example (Figure 1) and the results we observed in simulation studies (Figure 4, Panel c).

6 Discussion

6.1 Multiple testing with side information

Multiple testing with side or auxiliary information is an important topic that has received much attention recently. The research directions are wide-ranging as there are various types of side information, which may be either extracted from the same data using carefully constructed auxiliary sequences or gleaned from secondary data sources such as prior studies,

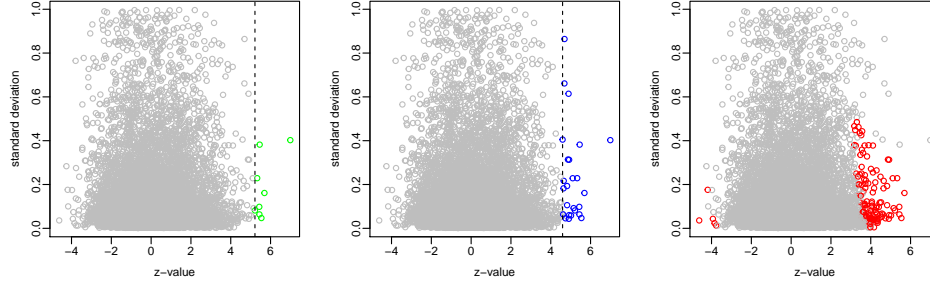


Figure 7: Scatter plot of rejected hypotheses by each method. Green: BH, blue: AZ, red: HART. AZ and BH reject every hypothesis to the right of the dashed line. The rejection region for HART depends on both z and σ .

domain-specific knowledge, structural constraints and external covariates. The recent works by Xia et al. (2019), Li and Barber (2019) and Cai et al. (2019) have focused on utilizing side information that encodes the *sparsity structure*. By contrast, our work investigates the impact of the *alternative distribution*, showing that incorporating σ_i can be extremely useful for improving the ranking and power in multiple testing.

In the context of FDR analysis, the key issue is that the hypotheses become unequal in light of side information. Efron (2008a) argued that ignoring the heterogeneity among study units may lead to FDR rules that are inefficient, noninterpretable and even invalid. We discuss two lines of work to further put our main contributions in context and to guide future research developments.

Grouping, pioneered by Efron (2008a), provides an effective strategy for capturing the heterogeneity in the data. Cai and Sun (2009) showed that the power of FDR procedures can be much improved by utilizing new ranking statistics adjusted for grouping. Recent works along this direction, including Liu et al. (2016), Barber and Ramdas (2017) and Sarkar and Zhao (2017), develop general frameworks for dealing with a class of hierarchical and grouping structures. However, the groups can be characterized in many ways and the optimal grouping strategy still remains unknown. Moreover, discretizing a continuous covariate by grouping leads to loss of information. HART directly incorporates σ_i into the ranking statistic and hence eliminates the need to define groups.

Weighting is another widely used strategy for incorporating side information into FDR analyses (Benjamini and Hochberg, 1997; Genovese et al., 2006; Roquain and Van De Wiel,

2009; Basu et al., 2018). For example, when the sparsity structure is encoded by a covariate sequence, weighted p -values can be constructed to up-weight the tests at coordinates where signals appear to be more frequent (Hu et al., 2012; Xia et al., 2019; Li and Barber, 2019). However, the derivation of weighting functions for directly incorporating heteroscedasticity seems to be rather complicated (Peña et al., 2011; Habiger et al., 2017). Notably, Habiger (2017) developed novel weights for p -values as functions of a class of auxiliary parameters, including σ_i as a special case, for a generic two-group mixture model. However, the formulation is complicated and the weights are hard to compute – the methodology requires handling the derivative of the power function, estimating several unknown quantities and tuning a host of parameters.

The works by Ignatiadis et al. (2016) and Lei and Fithian (2018) suggest that heterogeneous variances can be incorporated into inference as one type of side information. [Similar ideas were also included in earlier works by Efron (2008a) and Cai and Sun (2009) in their analyses of the school data.] However, because the variance issue is not the focus of their work, the discussions in Ignatiadis et al. (2016) and Lei and Fithian (2018) are very brief and it is unclear to us how to implement their proposals. They did not provide numerical evidence to illustrate whether or why incorporating the variances is beneficial. To the best of our knowledge, our work is the first to provide intuitive illustrations, clear evidence and novel insights on why heteroscedasticity is useful in large-scale inference (Section 2.2). The message is crucial as standardization has been a common practice in multiple testing. In contrast with existing works, HART provides a simple and powerful approach for adjusting heteroscedasticity with proven validity and optimality properties.

6.2 Open issues and future directions

We conclude the article by discussing several open issues. First, HART works better for large-scale problems where the density with heteroscedastic errors can be well estimated. For problems with several hundred tests or less, p -value based algorithms such as BH or the WAMDF approach (Habiger, 2017) are more suitable. The other promising direction for dealing with smaller-scale problems, suggested by Castillo and Roquain (2018), is to employ spike and slab priors to produce more stable empirical Bayes estimates (with frequentist guarantees under certain conditions). Second, in practice the model given by (2.2) can be

extended to

$$\mu_i|\sigma_i \stackrel{ind}{\sim} (1 - \pi_{\sigma_i})\delta_0(\cdot) + \pi_{\sigma_i}g_\mu(\cdot|\sigma_i), \quad \sigma_i^2 \stackrel{iid}{\sim} g_\sigma(\cdot), \quad (6.1)$$

where both the sparsity level and distribution of non-null effects depend on σ_i ; this setting has been considered in a closely related work by Weinstein et al. (2018). The heterogeneity-adjusted statistic is then given by

$$T_i = \mathbb{P}(\theta_i = 0|x_i, \sigma_i) = \frac{(1 - \pi_{\sigma_i})f_{0,\sigma_i}(x_i)}{f_{\sigma_i}(x_i)}, \quad (6.2)$$

where the varying proportion π_{σ_i} indicates that σ_i also captures the sparsity structure. This is possible, for example, in applications where observations from the alternative have larger variances compared to those from the null. An interesting, but challenging, direction for future research is to develop methodologies that can simultaneously incorporate both the sparsity and heterocedasticity structures into inference. Third, the HART-type methodology can only handle one covariate sequence $\{\sigma_i : 1 \leq i \leq m\}$. It would be of great interest to develop new methodologies and principles for information pooling for multiple testing with several covariate sequences. Finally, our work has assumed that σ_i are known in order to illustrate the key message (i.e. the impact of alternative distribution on the power of FDR analyses). Although this is a common practice, it is desirable to carefully investigate the impact of estimating σ_i on the accuracy and stability of large-scale inference.

References

- Barber, R. F. and Ramdas, A. (2017). The p-filter: multilayer false discovery rate control for grouped hypotheses. *Journal of the Royal Statistical Society: Series B (Statistical Methodology)*, 79(4):1247–1268.
- Basu, P., Cai, T. T., Das, K., and Sun, W. (2018). Weighted false discovery rate control in large-scale multiple testing. *Journal of the American Statistical Association*, 113:1172–1183.
- Benjamini, Y. and Hochberg, Y. (1995). Controlling the false discovery rate: a practical and powerful approach to multiple testing. *J. Roy. Statist. Soc. B*, 57:289–300.

- Benjamini, Y. and Hochberg, Y. (1997). Multiple hypotheses testing with weights. *Scandinavian Journal of Statistics*, **24**:407–418.
- Benjamini, Y. and Hochberg, Y. (2000). On the adaptive control of the false discovery rate in multiple testing with independent statistics. *Journal of Educational and Behavioral Statistics*, **25**:60–83.
- Brown, L. D. and Greenshtein, E. (2009). Nonparametric empirical bayes and compound decision approaches to estimation of a high-dimensional vector of normal means. *Annals of Statistics*, 37(4):1685–1704.
- Cai, T. T. and Sun, W. (2009). Simultaneous testing of grouped hypotheses: Finding needles in multiple haystacks. *J. Amer. Statist. Assoc.*, 104:1467–1481.
- Cai, T. T., Sun, W., and Wang, W. (2019). Cars: covariate assisted ranking and screening for large-scale two-sample inference (with discussion). *Journal of the Royal Statistical Society: Series B (Statistical Methodology)*, 81:187–234.
- Cao, H., Sun, W., and Kosorok, M. R. (2013). The optimal power puzzle: scrutiny of the monotone likelihood ratio assumption in multiple testing. *Biometrika*, 100(2):495–502.
- Castillo, I. and Roquain, E. (2018). On spike and slab empirical bayes multiple testing. *arXiv:1808.09748*.
- Donoho, D. and Jin, J. (2004). Higher criticism for detecting sparse heterogeneous mixtures. *Ann. Statist.*, 32:962–994.
- Dudoit, S., Shaffer, J. P., and Boldrick, J. C. (2003). Multiple hypothesis testing in microarray experiments. *Statist. Sci.*, 18(1):71–103.
- Efron, B. (2004a). Large-scale simultaneous hypothesis testing: the choice of a null hypothesis. *Journal of the American Statistical Association*, 99(465):96–104.
- Efron, B. (2004b). Large-scale simultaneous hypothesis testing: the choice of a null hypothesis. *J. Amer. Statist. Assoc.*, 99(465):96–104.
- Efron, B. (2007). Size, power and false discovery rates. *Ann. Statist.*, **35**:1351–1377.

- Efron, B. (2008a). Microarrays, empirical Bayes and the two-groups model. *Statist. Sci.*, **23**:1–22.
- Efron, B. (2008b). Simultaneous inference: When should hypothesis testing problems be combined? *Ann. Appl. Stat.*, **2**:197–223.
- Efron, B. (2011). Tweedie’s formula and selection bias. *Journal of the American Statistical Association*, 106(496):1602–1614.
- Efron, B., Tibshirani, R., Storey, J. D., and Tusher, V. (2001). Empirical Bayes analysis of a microarray experiment. *J. Amer. Statist. Assoc.*, 96:1151–1160.
- Fu, L., James, G., and Sun, W. (2018). Nonparametric empirical bayes estimation on heterogeneous data. Available at <http://www-bcf.usc.edu/~wenguans/Papers/NEST.html>.
- Genovese, C. and Wasserman, L. (2002). Operating characteristics and extensions of the false discovery rate procedure. *J. R. Stat. Soc. B*, **64**:499–517.
- Genovese, C. R., Roeder, K., and Wasserman, L. (2006). False discovery control with p-value weighting. *Biometrika*, 93(3):509–524.
- Habiger, J., Watts, D., and Anderson, M. (2017). Multiple testing with heterogeneous multinomial distributions. *Biometrics*, 73(2):562–570.
- Habiger, J. D. (2017). Adaptive false discovery rate control for heterogeneous data. *Statistica Sinica*, pages 1731–1756.
- Harvey, C. R. and Liu, Y. (2015). Backtesting. *The Journal of Portfolio Management*, 42(1):13–28.
- Holm, S. (1979). A simple sequentially rejective multiple test procedure. *Scandinavian journal of statistics*, 6:65–70.
- Hu, J. X., Zhao, H., and Zhou, H. H. (2012). False discovery rate control with groups. *Journal of the American Statistical Association*, 105:1215–1227.

- Ignatiadis, N., Klaus, B., Zaugg, J. B., and Huber, W. (2016). Data-driven hypothesis weighting increases detection power in genome-scale multiple testing. *Nature methods*, 13(7):577.
- Jin, J. and Cai, T. T. (2007). Estimating the null and the proportional of nonnull effects in large-scale multiple comparisons. *J. Amer. Statist. Assoc.*, **102**:495–506.
- Lei, L. and Fithian, W. (2018). Adapt: an interactive procedure for multiple testing with side information. *Journal of the Royal Statistical Society: Series B (Statistical Methodology)*, 80(4):649–679.
- Li, A. and Barber, R. F. (2019). Multiple testing with the structure-adaptive benjamini–hochberg algorithm. *Journal of the Royal Statistical Society: Series B (Statistical Methodology)*, 81(1):45–74.
- Liu, Y., Sarkar, S. K., and Zhao, Z. (2016). A new approach to multiple testing of grouped hypotheses. *Journal of Statistical Planning and Inference*, 179:1–14.
- Miller, C., Genovese, C., Nichol, R., Wasserman, L., Connolly, A., Reichart, D., Hopkins, D., Schneider, J., and Moore, A. (2001). Controlling the false-discovery rate in astrophysical data analysis. *Astronomical Journal*, **122**:3492–3505.
- Newton, M. A., Noueiry, A., Sarkar, D., and Ahlquist, P. (2004). Detecting differential gene expression with a semiparametric hierarchical mixture method. *Biostatistics*, 5(2):155–176.
- Pacifico, M., Genovese, C., Verdinelli, I., and Wasserman, L. (2004). False discovery control for random fields. *Journal of the American Statistical Association*, 99(468):1002–1014.
- Peña, E. A., Habiger, J. D., and Wu, W. (2011). Power-enhanced multiple decision functions controlling family-wise error and false discovery rates. *Annals of statistics*, 39(1):556.
- Roquain, E. and Van De Wiel, M. A. (2009). Optimal weighting for false discovery rate control. *Electronic journal of statistics*, 3:678–711.
- Sarkar, S. K. (2002). Some results on false discovery rate in stepwise multiple testing procedures. *Ann. Statist.*, 30:239–257.

- Sarkar, S. K. and Zhao, Z. (2017). Local false discovery rate based methods for multiple testing of one-way classified hypotheses. *arXiv:1712.05014*.
- Schwartzman, A., Dougherty, R. F., and Taylor, J. E. (2008). False discovery rate analysis of brain diffusion direction maps. *Ann. Appl. Stat.*, 2(1):153–175.
- Silverman, B. W. (1986). *Density estimation for statistics and data analysis*, volume 26. CRC press.
- Storey, J. D. (2002). A direct approach to false discovery rates. *J. Roy. Statist. Soc. B*, 64:479–498.
- Storey, J. D., Taylor, J. E., and Siegmund, D. (2004). Strong control, conservative point estimation and simultaneous conservative consistency of false discovery rates: a unified approach. *J. Roy. Statist. Soc. B*, 66(1):187–205.
- Sun, W. and Cai, T. T. (2007). Oracle and adaptive compound decision rules for false discovery rate control. *J. Amer. Statist. Assoc.*, 102:901–912.
- Sun, W. and McLain, A. C. (2012). Multiple testing of composite null hypotheses in heteroscedastic models. *Journal of the American Statistical Association*, 107(498):673–687.
- Sun, W. and Wei, Z. (2011). Large-scale multiple testing for pattern identification, with applications to time-course microarray experiments. *J. Amer. Statist. Assoc.*, 106:73–88.
- Taylor, J., Tibshirani, R., and Efron, B. (2005). The “miss rate” for the analysis of gene expression data. *Biostatistics*, 6(1):111–117.
- Tian, E., Zhan, F., Walker, R., Rasmussen, E., Ma, Y., Barlogie, B., and Shaughnessy, J. D. (2003). The role of the wnt-signaling antagonist dkk1 in the development of osteolytic lesions in multiple myeloma. *New England Journal of Medicine*, 349(26):2483–2494. PMID: 14695408.
- Tusher, V. G., Tibshirani, R., and Chu, G. (2001). Significance analysis of microarrays applied to the ionizing radiation response. *Proc. Natl. Acad. Sci. U. S. A.*, 98(9):5116–5121.

- Wand, M. P. and Jones, M. C. (1994). *Kernel Smoothing*, volume 60 of *Chapman and Hall CRC Monographs on Statistics and Applied Probability*. Chapman and Hall CRC.
- Weinstein, A., Ma, Z., Brown, L. D., and Zhang, C.-H. (2018). Group-linear empirical Bayes estimates for a heteroscedastic normal mean. *Journal of the American Statistical Association*, 113:698–710.
- Xia, Y., Cai, T. T., and Sun, W. (2019). Gap: A general framework for information pooling in two-sample sparse inference. *Journal of the American Statistical Association*, (just-accepted):to appear.
- Xie, X., Kou, S., and Brown, L. D. (2012). Sure estimates for a heteroscedastic hierarchical model. *Journal of the American Statistical Association*, 107(500):1465–1479.
- Zhao, Z., De Stefani, L., Zraggen, E., Binnig, C., Upfal, E., and Kraska, T. (2017). Controlling false discoveries during interactive data exploration. In *Proceedings of the 2017 ACM International Conference on Management of Data*, SIGMOD ’17, pages 527–540, New York, NY, USA. ACM.

Supplementary Material for “Information Loss and Power Distortion from Standardizing in Multiple Hypothesis Testing”

A Formulas for the Illustrative Example

Consider Model 2.8 in Section 2.2. We derive the formulas for the oracle p -value, oracle z -value and oracle full data procedures.

- δ^p corresponds to the thresholding rule $I(|Z_i| > t_p)$, where

$$t_p = \inf \left\{ t > 0 : \frac{2(1-\pi)\tilde{\Phi}(t)}{2(1-\pi)\tilde{\Phi}(t) + \pi \int \left\{ \tilde{\Phi}(t + \frac{\mu_a}{\sigma}) + \tilde{\Phi}(t - \frac{\mu_a}{\sigma}) \right\} dG(\sigma)} \leq \alpha \right\},$$

with $\tilde{\Phi}$ being the survival function of the $N(0, 1)$ variable.

- δ^z is a one-sided thresholding rule of the form $I(Z_i > t_z)$, where

$$t_z = \inf \left\{ t > 0 : \frac{(1-\pi)\tilde{\Phi}(t)}{(1-\pi)\tilde{\Phi}(t) + \pi \int \tilde{\Phi}(t - \frac{\mu_a}{\sigma}) dG(\sigma)} \leq \alpha \right\}.$$

- δ^{full} is of the form $I\{\mathbb{P}(\theta_i = 0|x_i, \sigma_i) < \lambda\}$. It can be written as $I\{Z_i > t_{z,\sigma}(\lambda)\}$, where

$$t_{z,\sigma}(\lambda) = \frac{\mu_a^2 - 2\sigma^2 \log \left\{ \frac{\lambda\pi}{(1-\lambda)(1-\pi)} \right\}}{2\mu_a\sigma}.$$

Denote λ^* the optimal threshold. Hence δ^{full} is given by $I\{P(\theta_i = 0|x_i, \sigma_i) < \lambda^*\}$, where

$$\lambda^* = \sup \left[\lambda \in [0, 1] : \frac{(1-\pi) \int \tilde{\Phi}\{t_{z,\sigma}(\lambda)\} dG(\sigma)}{(1-\pi) \int \tilde{\Phi}\{t_{z,\sigma}(\lambda)\} dG(\sigma) + \pi \int \tilde{\Phi}\{t_{z,\sigma}(\lambda) - \frac{\mu_a}{\sigma}\} dG(\sigma)} \right].$$

The optimal cutoffs can be solved numerically from the above. The powers are given

by

$$\begin{aligned}
AP(\boldsymbol{\delta}^p) &= \int \left\{ \tilde{\Phi}\left(t_p + \frac{\mu_a}{\sigma}\right) + \tilde{\Phi}\left(t_p - \frac{\mu_a}{\sigma}\right) \right\} dG(\sigma), \\
AP(\boldsymbol{\delta}^z) &= \int \tilde{\Phi}\left(t - \frac{\mu_a}{\sigma}\right) dG(\sigma), \\
AP(\boldsymbol{\delta}^{\text{full}}) &= \int \tilde{\Phi}\left\{t_{z,\sigma}(\lambda) - \frac{\mu_a}{\sigma}\right\} dG(\sigma).
\end{aligned}$$

B Proofs of Theorems

B.1 Proof of Theorem 1

We divide the proof into two parts. In Part (a), we establish two properties of the testing rule $\boldsymbol{\delta}^{\text{full}}(t) = \{\mathbb{I}(T_i < t) : 1 \leq i \leq m\}$ for an arbitrary $0 < t < 1$. In Part (b) we show that the oracle rule $\boldsymbol{\delta}^{\text{full}}(t^*)$ attains the mFDR level exactly and is optimal amongst all FDR procedures at level α .

Part (a). Denote $\alpha(t)$ the mFDR level of $\boldsymbol{\delta}^{\text{full}}(t)$. We shall show that (i) $\alpha(t) < t$ for all $0 < t < 1$ and that (ii) $\alpha(t)$ is nondecreasing in t . Note that $\mathbb{E}\{\sum_{i=1}^m (1 - \theta_i)\delta_i\} = \mathbb{E}_{\mathbf{X}, \boldsymbol{\sigma}}(\sum_{i=1}^m T_i \delta_i)$. According to the definition of $\alpha(t)$, we have

$$\mathbb{E}_{\mathbf{X}, \boldsymbol{\sigma}} \left\{ \sum_{i=1}^m \{T_i - \alpha(t)\} \mathbb{I}(T_i \leq t) \right\} = 0. \quad (\text{B.1})$$

We claim that $\alpha(t) < t$. Otherwise if $\alpha(t) \geq t$, then we must have $T_i < t \leq \alpha(t)$. It follows that the LHS must be negative, contradicting (B.1).

Next we show (ii). Let $\alpha(t_j) = \alpha_j$. We claim that if $t_1 < t_2$, then we must have $\alpha_1 \leq \alpha_2$. We argue by contradiction. Suppose that $t_1 < t_2$ but $\alpha_1 > \alpha_2$. Then

$$\begin{aligned}
(T_i - \alpha_2)\mathbb{I}(T_i < t_2) &= (T_i - \alpha_1)\mathbb{I}(T_i < t_1) + (\alpha_1 - \alpha_2)\mathbb{I}(T_i < t_1) + (T_i - \alpha_2)\mathbb{I}(t_1 \leq T_i < t_2) \\
&\geq (T_i - \alpha_1)\mathbb{I}(T_i < t_1) + (\alpha_1 - \alpha_2)\mathbb{I}(T_i < t_1) + (T_i - \alpha_1)\mathbb{I}(t_1 \leq T_i < t_2).
\end{aligned}$$

It follows that $\mathbb{E}\{\sum_{i=1}^m (T_i - \alpha_2)\mathbb{I}(T_i < t_2)\} > 0$ since $\mathbb{E}\{\sum_{i=1}^m (T_i - \alpha_1)\mathbb{I}(T_i < t_1)\} = 0$ according to (B.1), $\alpha_1 > \alpha_2$ and $T_i \geq t_1 > \alpha_1$, contradicting (B.1). Hence we must have $\alpha_1 < \alpha_2$.

Part (b). Let $\bar{\alpha} = \alpha(1)$. In Part (a), we show that $\alpha(t)$ is non-decreasing in t . It follows that for all $\alpha < \bar{\alpha}$, there exists a t^* such that $t^* = \sup\{t : \alpha(t^*) = \alpha\}$. By definition, t^* is the oracle threshold. Consider an arbitrary decision rule $\mathbf{d} = (d_1, \dots, d_m) \in \{0, 1\}^m$ such that $\text{mFDR}(\mathbf{d}) \leq \alpha$. We have $\mathbb{E} \left\{ \sum_{i=1}^m (T_i - \alpha) \delta_i^{full} \right\} = 0$ and $\mathbb{E} \left\{ \sum_{i=1}^m (T_i - \alpha) d_i \right\} \leq 0$. Hence

$$\mathbb{E} \left\{ \sum_{i=1}^m (\delta_i^{full} - d_i)(T_i - \alpha) \right\} \geq 0. \quad (\text{B.2})$$

Consider transformation $f(x) = (x - \alpha)/(1 - x)$. Note that $f(x)$ is monotone, we rewrite $\delta_i^{full} = \mathbb{I}[\{(T_i - \alpha)/(1 - T_i)\} < \lambda]$, where $\lambda = (t^* - \alpha)/(1 - t^*)$. In Part (a) we have shown that $\alpha < t_{OR} < 1$, which implies that $\lambda > 0$. Hence

$$\mathbb{E} \left[\sum_{i=1}^m (\delta_i^{full} - d_i) \{(T_i - \alpha) - \lambda(1 - T_i)\} \right] \leq 0. \quad (\text{B.3})$$

To see this, consider the terms where $\delta_i^{full} - d_i \neq 0$. Then we have two situations: (i) $\delta_i^{full} > d_i$ or (ii) $\delta_i^{full} < d_i$. In situation (i), $\delta_i^{full} = 1$, implying that $\{(T_i - \alpha)/(1 - T_i)\} < \lambda$. In situation (ii), $\delta_i^{full} = 0$, implying that $\{(T_i - \alpha)/(1 - T_i)\} \geq \lambda$. Therefore we always have $(\delta_i^{full} - d_i) \{(T_i - \alpha) - \lambda(1 - T_i)\} \leq 0$. Summing over the m terms and taking the expectation yield (B.3). Combining (B.2) and (B.3), we obtain

$$0 \leq \mathbb{E} \left\{ \sum_{i=1}^m (\delta_i^{full} - d_i)(T_i - \alpha) \right\} \leq \lambda \mathbb{E} \left\{ \sum_{i=1}^m (\delta_i^{full} - d_i)(T_i - \alpha) \right\}.$$

Finally, since $\lambda > 0$, it follows that $\mathbb{E} \left\{ \sum_{i=1}^m (\delta_i^{full} - d_i)(T_i - \alpha) \right\} > 0$. Finally, we apply the definition of ETP to conclude that $\text{ETP}(\boldsymbol{\delta}^{full}) \geq \text{ETP}(\mathbf{d})$ for all $\mathbf{d} \in \mathcal{D}_\alpha$.

B.2 Proof of Theorem 2

We begin with a summary of notation used throughout the proof:

- $Q(t) = m^{-1} \sum_{i=1}^m (T_i - \alpha) \mathbb{I}\{T_i < t\}$.
- $\hat{Q}(t) = m^{-1} \sum_{i=1}^m (\hat{T}_i - \alpha) \mathbb{I}\{\hat{T}_i < t\}$.
- $Q_\infty(t) = E\{(T_{OR} - \alpha) \mathbb{I}\{T_{OR} < t\}\}$.
- $t_\infty = \sup\{t \in (0, 1) : Q_\infty(t) \leq 0\}$: the “ideal” threshold.

For $T_{OR}^{(k)} < t < T_{OR}^{(k+1)}$, define a continuous version of $\widehat{Q}(t)$ as

$$\widehat{Q}_C(t) = \frac{t - \widehat{T}_{OR}^{(k)}}{\widehat{T}_{OR}^{(k+1)} - \widehat{T}_{OR}^{(k)}} \widehat{Q}_k + \frac{\widehat{T}_{OR}^{(k+1)} - t}{\widehat{T}_{OR}^{(k+1)} - \widehat{T}_{OR}^{(k)}} \widehat{Q}_{k+1},$$

where $\widehat{Q}_k = \widehat{Q}(\widehat{T}_{OR}^{(k)})$. Since $\widehat{Q}_C(t)$ is continuous and monotone, its inverse \widehat{Q}_C^{-1} is well-defined, continuous and monotone. Next we show the following two results in turn: (i) $\widehat{Q}(t) \xrightarrow{P} Q_\infty(t)$ and (ii) $\widehat{Q}_C^{-1}(0) \xrightarrow{P} t_\infty$.

To show (i), note that $Q(t) \xrightarrow{P} Q_\infty(t)$ by the WLLN, so that we only need to establish that $\widehat{Q}(t) - Q(t) \xrightarrow{P} 0$. We need the following lemma, which is proven in Section D.

Lemma 1 *Let $U_i = (T_i - \alpha)\mathbb{I}(T_i < t)$ and $\widehat{U}_i = (\widehat{T}_i - \alpha)\mathbb{I}\{\widehat{T}_i < t\}$. Then $\mathbb{E}(\widehat{U}_i - U_i)^2 = o(1)$.*

By Lemma 1 and Cauchy-Schwartz inequality, $\mathbb{E}\left\{(\widehat{U}_i - U_i)(\widehat{U}_j - U_j)\right\} = o(1)$. Let $S_m = \sum_{i=1}^m (\widehat{U}_i - U_i)$. It follows that

$$\text{Var}(m^{-1}S_m) \leq m^{-2} \sum_{i=1}^m \mathbb{E}\left\{(\widehat{U}_i - U_i)^2\right\} + O\left(\frac{1}{m^2} \sum_{i,j:i \neq j} \mathbb{E}\left\{(\widehat{U}_i - U_i)(\widehat{U}_j - U_j)\right\}\right) = o(1).$$

By Proposition 1, $\mathbb{E}(m^{-1}S_m) \rightarrow 0$, applying Chebyshev's inequality, we obtain $m^{-1}S_m = \widehat{Q}(t) - Q(t) \xrightarrow{P} 0$. Hence (i) is proved. Notice that $Q_\infty(t)$ is continuous by construction, we also have $\widehat{Q}(t) \xrightarrow{P} \widehat{Q}_C(t)$.

Next we show (ii). Since $\widehat{Q}_C(t)$ is continuous, for any $\varepsilon > 0$, we can find $\eta > 0$ such that $\left|\widehat{Q}_C^{-1}(0) - \widehat{Q}_C^{-1}\left\{\widehat{Q}_C(t_\infty)\right\}\right| < \varepsilon$ if $\left|\widehat{Q}_C(t_\infty)\right| < \eta$. It follows that

$$P\left\{\left|\widehat{Q}_C(t_\infty)\right| > \eta\right\} \geq P\left\{\left|\widehat{Q}_C^{-1}(0) - \widehat{Q}_C^{-1}\left\{\widehat{Q}_C(t_\infty)\right\}\right| > \varepsilon\right\}.$$

Proposition 1 and the WLLN imply that $\widehat{Q}_C(t) \xrightarrow{P} Q_\infty(t)$. Note that $Q_\infty(t_\infty) = 0$. Then $P\left(\left|\widehat{Q}_C(t_\infty)\right| > \eta\right) \rightarrow 0$. Hence we have $\widehat{Q}_C^{-1}(0) \xrightarrow{P} \widehat{Q}_C^{-1}\left\{\widehat{Q}_C(t_\infty)\right\} = t_\infty$, completing the proof of (ii).

To show $\text{FDR}(\boldsymbol{\delta}^{dd}) = \text{FDR}(\boldsymbol{\delta}^{full}) + o(1) = \alpha + o(1)$, we only need to show $\text{mFDR}(\boldsymbol{\delta}^{dd}) = \text{mFDR}(\boldsymbol{\delta}^{full}) + o(1)$. The result then follows from the asymptotic equivalence of FDR and mFDR, which was proven in Cai et al. (2019).

Define the continuous version of $Q(t)$ as $Q_C(t)$ and the corresponding threshold as $Q_C^{-1}(0)$. Then by construction, we have

$$\boldsymbol{\delta}^{dd} = [\mathbb{I}\{\hat{T}_i \leq \hat{Q}_C^{-1}(0)\} : 1 \leq i \leq m] \quad \text{and} \quad \boldsymbol{\delta}^{full} = [\mathbb{I}\{T_i \leq Q_C^{-1}(0)\} : 1 \leq i \leq m].$$

Following the previous arguments, we can show that $Q_C^{-1}(0) \xrightarrow{p} t_\infty$. It follows that $\hat{Q}_C^{-1}(0) = Q_C^{-1}(0) + o_p(1)$. By construction $\text{mFDR}(\boldsymbol{\delta}^{full}) = \alpha$. The mFDR level of $\boldsymbol{\delta}^{dd}$ is

$$\text{mFDR}(\boldsymbol{\delta}^{dd}) = \frac{P_{H_0} \left\{ \hat{T}_i \leq \hat{Q}_C^{-1}(0) \right\}}{P \left\{ \hat{T}_i \leq \hat{Q}_C^{-1}(0) \right\}}.$$

From Proposition 2, $\hat{T}_i \xrightarrow{p} T_i$. Using the continuous mapping theorem, $\text{mFDR}(\boldsymbol{\delta}^{dd}) = \text{mFDR}(\boldsymbol{\delta}^{full}) + o(1) = \alpha + o(1)$. The desired result follows.

Finally, using the fact that $\hat{T}_i \xrightarrow{p} T_i$ and $\hat{Q}_C^{-1}(0) \xrightarrow{p} Q_C^{-1}(0)$, we can similarly show that

$$\text{ETP}(\boldsymbol{\delta}^{dd})/\text{ETP}(\boldsymbol{\delta}^{full}) = 1 + o(1).$$

C Proof of Proposition 1

Summary of notation

The following notation will be used throughout the proofs:

- $\hat{f}_\sigma^*(x) = \sum_{j=1}^m \left\{ \frac{\phi_{h_\sigma}(\sigma - \sigma_j)}{\sum_{i=1}^m \phi_{h_\sigma}(\sigma - \sigma_i)} \right\} \phi_{h_x \sigma_j}(x - x_j).$
- $\hat{f}_{1,\sigma}^*(x) = \sum_{j=1}^m \left\{ \frac{\phi_{h_\sigma}(\sigma - \sigma_j) \mathbb{I}(\theta_j = 1)}{\sum_{i=1}^m \phi_{h_\sigma}(\sigma - \sigma_i) \mathbb{I}(\theta_i = 1)} \right\} \phi_{h_x \sigma_j}(x - x_j).$
- $\tilde{f}_{1,\sigma}(x) = \sum_{j=1}^m \left\{ \frac{\phi_{h_\sigma}(\sigma - \sigma_j) P(\theta_j = 1 | x_j, \sigma_j)}{\sum_{i=1}^m \phi_{h_\sigma}(\sigma - \sigma_i) P(\theta_i = 1 | x_i, \sigma_i)} \right\} \phi_{h_x \sigma_j}(x - x_j).$
- $\hat{f}_{1,\sigma}(x) = \sum_{j=1}^m \left\{ \frac{\phi_{h_\sigma}(\sigma - \sigma_j) \hat{P}(\theta_j = 1 | x_j, \sigma_j)}{\sum_{i=1}^m \phi_{h_\sigma}(\sigma - \sigma_i) \hat{P}(\theta_i = 1 | x_i, \sigma_i)} \right\} \phi_{h_x \sigma_j}(x - x_j).$
- $\hat{f}_\sigma(x) = (1 - \hat{\pi}) f_{0,\sigma}(x) + \hat{\pi} \hat{f}_{1,\sigma}(x).$

The basic idea is that a consistent one-step estimator constructed via $\hat{f}_\sigma^*(x)$ leads to a consistent two-step estimator via $\hat{f}_\sigma(x)$. By Condition (C4) and the triangle inequality, it

is sufficient to show that

$$\mathbb{E} \int \left\{ \hat{f}_{1,\sigma}(x) - f_{1,\sigma}(x) \right\}^2 dx \rightarrow 0. \quad (\text{C.4})$$

Let $u_j = \frac{\phi_{h_\sigma}(\sigma - \sigma_j)}{\sum_{i=1}^m \phi_{h_\sigma}(\sigma - \sigma_i)}$. A direct consequence of condition (C1) is $0 < \frac{C_1}{m} \leq u_j \leq \frac{C_2}{m} < \infty$ for some positive constants C_1 and C_2 . Let $C' = \min(1, C_1)$. Consider event

$$\mathcal{A} = \left\{ \left| \sum_{i=1}^m \theta_j - m\pi \right| < \frac{C'}{2} m\pi \right\}. \quad (\text{C.5})$$

By Hoeffding's inequality and Condition (C2), $P(\mathcal{A}^C)O(h_x^{-2}) \leq \exp(-C'^2 m/2)O(h_x^{-2}) \rightarrow 0$. Therefore it suffices to prove (C.4) under \mathcal{A} . We establish the result in three steps:

1. $\mathbb{E} \int \{\hat{f}_{1,\sigma}^*(x) - f_{1,\sigma}(x)\}^2 dx \rightarrow 0$.
2. $\mathbb{E} \int \{\tilde{f}_{1,\sigma}(x) - \hat{f}_{1,\sigma}^*(x)\}^2 dx \rightarrow 0$.
3. $\mathbb{E} \int \{\hat{f}_{1,\sigma}(x) - \tilde{f}_{1,\sigma}(x)\}^2 dx \rightarrow 0$.

The proposition then follows from the triangle inequality.

C.1 Proof of Step (a)

Let $b_j^* = \frac{\phi_{h_\sigma}(\sigma - \sigma_j)\mathbb{I}(\theta_j = 1)}{\sum_{i=1}^m \phi_{h_\sigma}(\sigma - \sigma_i)\mathbb{I}(\theta_i = 1)}$. It is easy to show that

$$\left\{ \hat{f}_{1,\sigma}^*(x) - f_{1,\sigma}(x) \right\}^2 = \sum_{j=1}^m \sum_{k=1}^m b_j^* b_k^* \{ \phi_{h_x \sigma_k}(x - x_k) - f_{1,\sigma}(x) \} \{ \phi_{h_x \sigma_j}(x - x_j) - f_{1,\sigma}(x) \}.$$

Under condition (C1) and event \mathcal{A} , we have $\mathbb{E}(b_j^* b_k^*) = O(m^{-2})$. Using standard arguments in density estimation theory (e.g. Wand and Jones (1994) page 21), we have $\mathbb{E} \int \{\hat{f}_{1,\sigma}^*(x) - f_{1,\sigma}(x)\}^2 dx = O\{(mh_x)^{-1} + h_x^4\}$. Under condition (C2) the RHS $\rightarrow 0$, establishing Step (a).

C.2 Proof of Step (b)

Let $b_j = \frac{\phi_{h_\sigma}(\sigma - \sigma_j)P(\theta_j = 1|x_j, \sigma_j)}{\sum_{i=1}^m \phi_{h_\sigma}(\sigma - \sigma_i)P(\theta_i = 1|x_i, \sigma_i)}$. Then

$$\begin{aligned} \left\{ \tilde{f}_{1,\sigma}(x) - \hat{f}_{1,\sigma}^*(x) \right\}^2 &= \sum_{j=1}^m (b_j^* - b_j)^2 \phi_{h_x \sigma_j}^2(x - x_j) \\ &\quad + \sum_{(j,k): j \neq k} (b_j^* - b_j)(b_k^* - b_k) \phi_{h_x \sigma_j}(x - x_j) \phi_{h_x \sigma_k}(x - x_k). \end{aligned} \quad (\text{C.6})$$

We first bound $\mathbb{E}(b_j^* - b_j)^2$. Write $\mathbb{E}(b_j^* - b_j)^2 = \{\mathbb{E}(b_j^* - b_j)\}^2 + \text{Var}(b_j^* - b_j)$. It is clear that $\mathbb{E}(b_j^*)$ and $\mathbb{E}(b_j)$ are both $O(m^{-1})$. Hence $\{\mathbb{E}(b_j^* - b_j)\}^2 = O(m^{-2})$. Next consider $\text{Var}(b_j^* - b_j) = \text{Var}(b_j^*) + \text{Var}(b_j) - 2\text{Cov}(b_j^*, b_j)$. We have

$$\text{Var}(b_j^*) = \text{Var} \left\{ \frac{\mathbb{I}(\theta_j = 1) \phi_{h_\sigma}(\sigma - \sigma_j)}{\sum_{i=1}^m \phi_{h_\sigma}(\sigma - \sigma_i) \mathbb{I}(\theta_i = 1)} \right\} \leq \mathbb{E} \left\{ \frac{\phi_{h_\sigma}(\sigma - \sigma_j)}{\sum_{i=1}^m \phi_{h_\sigma}(\sigma - \sigma_i) \mathbb{I}(\theta_i = 1)} \right\}^2 = O(m^{-2}).$$

Similarly $\text{Var}(b_j) = O(m^{-2})$. It follows that $\text{Cov}(b_j^*, b_j) = O(m^{-2})$. Therefore $\text{Var}(b_j^* - b_j) = O(m^{-2})$ and $\mathbb{E}(b_j^* - b_j)^2 = O(m^{-2})$. Using the fact that $\int \phi_{h_x \sigma_j}^2(x - x_j) dx = O(h_x^{-1})$, we have

$$\int \mathbb{E} \sum_{j=1}^m (b_j^* - b_j)^2 \phi_{h_x \sigma_j}^2(x - x_j) dx = O\{(mh_x)^{-1}\} \rightarrow 0. \quad (\text{C.7})$$

Next we bound $\mathbb{E}\{(b_j^* - b_j)(b_k^* - b_k)\}$ for $j \neq k$. Consider the decomposition

$$\mathbb{E}\{(b_j^* - b_j)(b_k^* - b_k)\} = \mathbb{E}(b_j^* - b_j) \mathbb{E}(b_k^* - b_k) + \text{Cov}(b_j^* - b_j, b_k^* - b_k). \quad (\text{C.8})$$

Our goal is show that $\mathbb{E}\{(b_j^* - b_j)(b_k^* - b_k)\} = O(m^{-3})$. It suffices to show

$$\mathbb{E}_{\theta|\sigma, \mathbf{x}}\{(b_j^* - b_j)(b_k^* - b_k)\} = O(m^{-3}). \quad (\text{C.9})$$

Observe that $\text{Var} \left\{ \frac{1}{mh_\sigma^{-1}} \sum_{i=1}^m \phi_{h_\sigma}(\sigma - \sigma_j) \mathbb{I}(\theta_i = 1) | \sigma, \mathbf{x} \right\} = O(m^{-1})$ and

$$\mathbb{E}_{\theta|\sigma, \mathbf{x}} \left\{ \frac{1}{mh_\sigma^{-1}} \sum_{i=1}^m \phi_{h_\sigma}(\sigma - \sigma_j) \mathbb{I}(\theta_i = 1) \right\} = \frac{1}{mh_\sigma^{-1}} \sum_{i=1}^m \phi_{h_\sigma}(\sigma - \sigma_j) P(\theta_i = 1 | \sigma_i, x_i).$$

Applying Chebyshev's inequality,

$$\frac{1}{mh_\sigma^{-1}} \sum_{i=1}^m \phi_{h_\sigma}(\sigma - \sigma_j) \mathbb{I}(\theta_i = 1) - \frac{1}{mh_\sigma^{-1}} \sum_{i=1}^m \phi_{h_\sigma}(\sigma - \sigma_j) P(\theta_i = 1 | \sigma_i, x_i) \xrightarrow{p} 0.$$

It follows that for any $\epsilon > 0$,

$$P \left\{ \left| \sum_{i=1}^m \phi_{h_\sigma}(\sigma - \sigma_j) \mathbb{I}(\theta_i = 1) - \sum_{i=1}^m \phi_{h_\sigma}(\sigma - \sigma_j) P(\theta_i = 1 | \sigma_i, x_i) \right| < \epsilon mh_\sigma^{-1} \right\} \rightarrow 1.$$

Under \mathcal{A} defined in (C.5), we have $\sum_{i=1}^m \phi_{h_\sigma}(\sigma - \sigma_j) \mathbb{I}(\theta_i = 1) > h_\sigma^{-1} C_3 m$ for some C_3 , and

$$P \left\{ \sum_{i=1}^m \phi_{h_\sigma}(\sigma - \sigma_j) P(\theta_i = 1 | \sigma_i, x_i) < h_\sigma^{-1} C_3 m \right\} \rightarrow 0. \quad (\text{C.10})$$

The boundedness of b_j^* and b_j and (C.10) imply that we only need to prove (C.9) on the event $\mathcal{A}^* = \{(\mathbf{x}, \boldsymbol{\sigma}) : \sum_{i=1}^m \phi_{h_\sigma}(\sigma - \sigma_j) P(\theta_i = 1 | \sigma_i, x_i) \geq h_\sigma^{-1} C_3 m\}$. We shall consider $\mathbb{E}_{\boldsymbol{\theta}|\boldsymbol{\sigma}, \mathbf{x}}(b_j^* - b_j)$ and $\text{Cov}(b_j^* - b_j, b_k^* - b_k | \boldsymbol{\sigma}, \mathbf{x})$ in turn. Write

$$\begin{aligned} \mathbb{E}_{\boldsymbol{\theta}|\boldsymbol{\sigma}, \mathbf{x}}(b_j^*) &= \mathbb{E}_{\boldsymbol{\theta}|\boldsymbol{\sigma}, \mathbf{x}} \left\{ \frac{\mathbb{I}(\theta_j = 1) \phi_{h_\sigma}(\sigma - \sigma_j)}{\sum_{i=1}^m \phi_{h_\sigma}(\sigma - \sigma_i) \mathbb{I}(\theta_i = 1)} \right\} \\ &= P(\theta_j = 1 | x_j, \sigma_j) \mathbb{E}_{\boldsymbol{\theta}|\boldsymbol{\sigma}, \mathbf{x}} \left\{ \frac{\phi_{h_\sigma}(\sigma - \sigma_j)}{\sum_{i=1}^m \phi_{h_\sigma}(\sigma - \sigma_i) \mathbb{I}(\theta_i = 1)} \right\} \\ &\quad + \text{Cov} \left\{ \theta_j, \frac{\phi_{h_\sigma}(\sigma - \sigma_j)}{\sum_{i=1}^m \phi_{h_\sigma}(\sigma - \sigma_i) \mathbb{I}(\theta_i = 1)} \middle| \boldsymbol{\sigma}, \mathbf{x} \right\}. \end{aligned}$$

Let $Y = \frac{\phi_{h_\sigma}(\sigma - \sigma_j)}{\sum_{i=1}^m \phi_{h_\sigma}(\sigma - \sigma_i) \mathbb{I}(\theta_i = 1)}$. We state three lemmas that are proven in Section D.

Lemma 2 *Under event \mathcal{A}^* , we have $\mathbb{E}_{\boldsymbol{\theta}|\boldsymbol{\sigma}, \mathbf{x}}(Y) - \mathbb{E}_{\boldsymbol{\theta}|\boldsymbol{\sigma}, \mathbf{x}}(Y | \theta_j = 1) = O(m^{-2})$ and $\mathbb{E}_{\boldsymbol{\theta}|\boldsymbol{\sigma}, \mathbf{x}}(Y) - \mathbb{E}_{\boldsymbol{\theta}|\boldsymbol{\sigma}, \mathbf{x}}(Y | \theta_j = 0) = O(m^{-2})$.*

Lemma 3 *Under event \mathcal{A}^* , we have*

$$\mathbb{E}_{\boldsymbol{\theta}|\boldsymbol{\sigma}, \mathbf{x}} \left\{ \frac{\phi_{h_\sigma}(\sigma - \sigma_j)}{\sum_{i=1}^m \phi_{h_\sigma}(\sigma - \sigma_i) \mathbb{I}(\theta_i = 1)} \right\} = \frac{\phi_{h_\sigma}(\sigma - \sigma_j)}{\sum_{i=1}^m \phi_{h_\sigma}(\sigma - \sigma_i) P(\theta_i = 1 | x_i, \sigma_i)} + O(m^{-2}).$$

Lemma 4 *Under event \mathcal{A}^* , we have $\text{Cov}(b_j^* - b_j, b_k^* - b_k | \boldsymbol{\sigma}, \mathbf{x}) = O(m^{-3})$.*

According to Lemma 2, we have

$$\begin{aligned}
& \text{Cov}\left\{\theta_j, \frac{\phi_{h_\sigma}(\sigma - \sigma_j)}{\sum_{i=1}^m \phi_{h_\sigma}(\sigma - \sigma_i) \mathbb{I}(\theta_i = 1)} \middle| \boldsymbol{\sigma}, \mathbf{x}\right\} \\
&= \int \{P(\theta_j = 0|x_j, \sigma_j)P(\theta_j = 1|x_j, \sigma_j)\} \{y - \mathbb{E}_{\boldsymbol{\theta}|\boldsymbol{\sigma}, \mathbf{x}}(Y)\} f_{Y|\theta_j=1, \boldsymbol{\sigma}, \mathbf{x}}(y) dy \\
&\quad - \int \{1 - P(\theta_j = 1|x_j, \sigma_j)\}^2 \{y - \mathbb{E}_{\boldsymbol{\theta}|\boldsymbol{\sigma}, \mathbf{x}}(Y)\} f_{Y|\theta_j=0, \boldsymbol{\sigma}, \mathbf{x}}(y) dy = O(m^{-2}).
\end{aligned} \tag{C.11}$$

Together with Lemma 3, we have

$$\mathbb{E}_{\boldsymbol{\theta}|\boldsymbol{\sigma}, \mathbf{x}} \left\{ \frac{\mathbb{I}(\theta_j = 1) \phi_{h_\sigma}(\sigma - \sigma_j)}{\sum_{i=1}^m \phi_{h_\sigma}(\sigma - \sigma_i) \mathbb{I}(\theta_i = 1)} \right\} = \frac{P(\theta_j = 1|x_j, \sigma_j) \phi_{h_\sigma}(\sigma - \sigma_j)}{\sum_{i=1}^m \phi_{h_\sigma}(\sigma - \sigma_i) P(\theta_i = 1|x_i, \sigma_i)} + O(m^{-2}). \tag{C.12}$$

It follows that $\mathbb{E}(b_j^* - b_j) = O(m^{-2})$ and $\mathbb{E}(b_j^* - b_j) \mathbb{E}(b_k^* - b_k) = O(m^{-4})$. The decomposition (C.8) and Lemma 4 together imply $\mathbb{E}\{(b_j^* - b_j)(b_k^* - b_k)\} = O(m^{-3})$. It follows that

$$\int \mathbb{E} \sum_{(j,k): j \neq k} (b_j^* - b_j)(b_k^* - b_k) \phi_{h_x \sigma_j}(x - x_j) \phi_{h_x \sigma_j}(x - x_k) dx = O\{(mh_x)^{-1}\} \rightarrow 0. \tag{C.13}$$

Combing (C.6), (C.7) and (C.13), we conclude that $\mathbb{E} \int \{\tilde{f}_{1,\sigma}(x) - \hat{f}_{1,\sigma}^*(x)\}^2 dx \rightarrow 0$.

C.3 Proof of Step (c)

Let $q_j = P(\theta_j = 1|\sigma_j, x_j)$, $\hat{q}_j = \hat{P}(\theta_j = 1|\sigma_j, x_j) = \min \left\{ \frac{(1 - \hat{\pi}) f_{0,\sigma_j}(x_j)}{\hat{f}_{\sigma_j}^*(x_j)}, 1 \right\}$ and $\hat{f}_{1,\sigma}(x) = \sum_{j=1}^m \frac{\phi_{h_\sigma}(\sigma - \sigma_j) \hat{q}_j}{\sum_{i=1}^m \phi_{h_\sigma}(\sigma - \sigma_i) \hat{q}_i} \phi_{h_x \sigma_j}(x - x_j)$.

Write $\hat{q}_j = q_j + a_j$, then $|a_j| \leq 1$ and $a_j = o_P(1)$. We have

$$\begin{aligned}
\mathbb{E} \int \left\{ \hat{f}_{1,\sigma}(x) - \tilde{f}_{1,\sigma}(x) \right\}^2 dx &= O \left\{ h_x^{-1} m^2 \mathbb{E} \left(\frac{\phi_{h_\sigma}(\sigma - \sigma_j) \hat{q}_j}{\sum_{i=1}^m \phi_{h_\sigma}(\sigma - \sigma_i) \hat{q}_i} - \frac{\phi_{h_\sigma}(\sigma - \sigma_j) q_j}{\sum_{i=1}^m \phi_{h_\sigma}(\sigma - \sigma_i) q_i} \right)^2 \right\} \\
&= O \{ h_x^{-1} h_\sigma^2 \mathbb{E} a_j^2 \}.
\end{aligned}$$

Next we explain why the last equality holds. Let $c_i = \phi_{h_\sigma}(\sigma - \sigma_i)h_\sigma$. Then

$$\begin{aligned}
& \mathbb{E} \left\{ \frac{\phi_{h_\sigma}(\sigma - \sigma_j)\hat{q}_j}{\sum_{i=1}^m \phi_{h_\sigma}(\sigma - \sigma_i)\hat{q}_i} - \frac{\phi_{h_\sigma}(\sigma - \sigma_j)q_j}{\sum_{i=1}^m \phi_{h_\sigma}(\sigma - \sigma_i)q_i} \right\}^2 \\
&= \mathbb{E} \left\{ \frac{a_j \sum_{i=1}^m \phi_{h_\sigma}(\sigma - \sigma_i)q_i - q_j \sum_{i=1}^m \phi_{h_\sigma}(\sigma - \sigma_i)a_i}{\{\sum_{i=1}^m \phi_{h_\sigma}(\sigma - \sigma_i)\hat{q}_i\}\{\sum_{i=1}^m \phi_{h_\sigma}(\sigma - \sigma_i)q_i\}} \right\}^2 \\
&= h_\sigma^2 \frac{1}{m^4} O \left[\mathbb{E} \left\{ a_j \sum_{i=1}^m c_i q_i - q_j \sum_{i=1}^m c_i a_i \right\}^2 \right] \\
&= \frac{h_\sigma^2}{m^4} O \left[\mathbb{E} \left\{ m^2 a_j^2 - 2ma_j \sum_{i=1}^m a_i + \left(\sum_{i=1}^m a_i \right)^2 \right\} \right] = \frac{h_\sigma^2}{m^2} O \{ \mathbb{E}(a_j^2) \}.
\end{aligned}$$

The last line holds by noting that $\mathbb{E}(a_j a_i) \leq \sqrt{\mathbb{E}(a_j^2)\mathbb{E}(a_i^2)} = O\{\mathbb{E}(a_j^2)\}$.

The next step is to bound $\mathbb{E}(a_j^2)$. Note that $a_j = O \left\{ \frac{f_{0,\sigma_j}(x_j)\{\hat{f}_{\sigma_j}^*(x_j) - f_{\sigma_j}(x_j)\}}{f_{\sigma_j}(x_j)\hat{f}_{\sigma_j}^*(x_j)} \right\}$.

By the construction of \hat{q}_j , we have $\hat{f}_{\sigma_j}(x_j) \geq (1 - \hat{\pi})f_{0,\sigma_j}(x_j)$. Hence

$$a_j = O \left\{ 1 - \frac{\hat{f}_{\sigma_j}^*(x_j)}{f_{\sigma_j}(x_j)} \right\} \quad \text{and} \quad \mathbb{E}(a_j^2) = O \left[\mathbb{E} \left\{ 1 - \frac{\hat{f}_{\sigma_j}^*(x_j)}{f_{\sigma_j}(x_j)} \right\}^2 \right].$$

Let $\mathcal{K}_j = \left(-\sigma_j\sqrt{\delta}\sqrt{\log m} - M, \sigma_j\sqrt{\delta}\sqrt{\log m} + M \right)$. By the Gaussian tail bound, $P\{x_j \notin \mathcal{K}_j\} = O(m^{-\delta/2})$. By the boundedness of a_j^2 and the fact that $h_x^{-1}h_\sigma^2 m^{-\delta/2} \rightarrow 0$ (Condition (C3)),

we only need to consider $\mathbb{E} \left[1 - 2\frac{\hat{f}_{\sigma_j}^*(x_j)}{f_{\sigma_j}(x_j)} + \left\{ \frac{\hat{f}_{\sigma_j}^*(x_j)}{f_{\sigma_j}(x_j)} \right\}^2 \middle| x_j \right]$ for $x_j \in \mathcal{K}_j$.

Let $f_\sigma(x) = \int \phi_\sigma(x) \{(1 - \pi)\delta_0(x_j - x) + \pi g_\mu(x_j - x)\} dx$. Define a jackknifed version of $\hat{f}_{\sigma_j}^{*,(j)}$ that is formed without the pair (σ_j, x_j) . It follows that

$$\mathbb{E}\{\hat{f}_{\sigma_j}^{*,(j)}(x_j)|x_j\} = \int \int \phi_{\sqrt{\sigma^2 + h_x^2 \sigma_j^2}}(x) \{(1 - \pi)\delta_0(x_j - x) + \pi g_\mu(x_j - x)\} g_\sigma(\sigma_j) d\sigma_j dx.$$

By the intermediate value theorem and Condition (C1),

$$\mathbb{E}\{\hat{f}_{\sigma_j}^{*,(j)}(x_j)|x_j\} = \int \phi_{\sqrt{\sigma^2 + h_x^2 c}}(x) \{(1 - \pi)\delta_0(x_j - x) + \pi g_\mu(x_j - x)\} dx$$

for some constant c . Next consider the ratio

$$\frac{\mathbb{E}\{\hat{f}_{\sigma_j}^{*,(j)}(x_j)|x_j\}}{f_{\sigma_j}(x_j)} = \frac{\int \phi_{\sqrt{\sigma^2+h_x^2c}}(x) \{(1-\pi)\delta_0(x_j-x) + \pi g_\mu(x_j-x)\} dx}{\int \phi_\sigma(x) \{(1-\pi)\delta_0(x_j-x) + \pi g_\mu(x_j-x)\} dx}.$$

By Condition (C1), $\text{supp}(g_\mu) \in (-M, M)$ with $M < \infty$, we have

$$\inf_{x_j-M < x < x_j+M} \frac{\phi_{\sqrt{\sigma^2+h_x^2c}}(x)}{\phi_\sigma(x)} \leq \frac{\mathbb{E}\{\hat{f}_{\sigma_j}^{*,(j)}(x_j)|x_j\}}{f_{\sigma_j}(x_j)} \leq \sup_{x_j-M < x < x_j+M} \frac{\phi_{\sqrt{\sigma^2+h_x^2c}}(x)}{\phi_\sigma(x)}.$$

Note that $x_j \in (-\sigma_j\sqrt{\delta}\sqrt{\log m} - M, \sigma_j\sqrt{\delta}\sqrt{\log m} + M)$. The above infimum and supremum are taken over $x \in \mathcal{K} = (-\sigma_j\sqrt{\delta}\sqrt{\log m} - 2M, \sigma_j\sqrt{\delta}\sqrt{\log m} + 2M)$. Using Taylor expansion

$$\frac{\phi_{\sqrt{\sigma^2+h_x^2c}}(x)}{\phi_\sigma(x)} = \frac{\sigma}{\sqrt{\sigma^2+h_x^2c}} \left[1 + \sum_{k=1}^{\infty} \frac{1}{k!} \left\{ \frac{h_x^2cx^2}{2(\sigma^2+h_x^2c)} \right\}^k \right],$$

we have $\inf_{x \in \mathcal{K}} \frac{\phi_{\sqrt{\sigma^2+h_x^2c}}(x)}{\phi_\sigma(x)} = \frac{\sigma}{\sqrt{\sigma^2+h_x^2c}} = 1 + O(h_x^2)$. Similarly,

$$\sup_{x \in \mathcal{K}} \frac{\sigma}{\sqrt{\sigma^2+h_x^2c}} \left\{ 1 + \sum_{k=1}^{\infty} \frac{1}{k!} \left(\frac{h_x^2cx^2}{2(\sigma^2+h_x^2c)} \right)^k \right\} = 1 + O(h_x^2) + O \left[\sup \sum_{k=1}^{\infty} \frac{1}{k!} \left\{ \frac{h_x^2cx^2}{2(\sigma^2+h_x^2c)} \right\}^k \right].$$

It follows that

$$\frac{\mathbb{E}\{\hat{f}_{\sigma_j}^{*,(j)}(x_j)|x_j\}}{f_{\sigma_j}(x_j)} = 1 + O(h_x^2) + O \left\{ \sup \sum_{k=1}^{\infty} \frac{1}{k!} \left(\frac{h_x^2cx^2}{2(\sigma^2+h_x^2c)} \right)^k \right\}, \quad (\text{C.14})$$

$$1 - 2 \frac{\mathbb{E}\{\hat{f}_{\sigma_j}^{*,(j)}(x_j)|x_j\}}{f_{\sigma_j}(x_j)} = -1 + O(h_x^2) + O \left\{ \sup \sum_{k=1}^{\infty} \frac{1}{k!} \left(\frac{h_x^2cx^2}{2(\sigma^2+h_x^2c)} \right)^k \right\}. \quad (\text{C.15})$$

Next consider $\mathbb{E} \left\{ \frac{\hat{f}_{\sigma_j}^{*,(j)}(x_j)}{f_{\sigma_j}(x_j)} \middle| x_j \right\}^2 = \left[\frac{\mathbb{E}\{\hat{f}_{\sigma_j}^{*,(j)}(x_j)|x_j\}}{f_{\sigma_j}(x_j)} \right]^2 + \text{Var} \left\{ \frac{\hat{f}_{\sigma_j}^{*,(j)}(x_j)}{f_{\sigma_j}(x_j)} \middle| x_j \right\}$. By the same computation on page 21 of Wand and Jones (1994),

$$\text{Var} \left\{ \frac{\hat{f}_{\sigma_j}^{*,(j)}(x_j)}{f_{\sigma_j}(x_j)} \middle| x_j \right\} = O \{ (mh_x)^{-1} f_{\sigma_j}(x_j)^{-1} \} + o \{ (mh_x)^{-1} f_{\sigma_j}(x_j)^{-2} \}.$$

Since $x_j \in \mathcal{K}_j$, $f_{\sigma_j}(x_j) \geq C_3 m^{-\delta/2}$ for some constant C_3 , together with Condition (C3), we

have $h_x^{-1} \text{Var} \left\{ \frac{\hat{f}_{\sigma_j}^{*,(j)}(x_j)}{f_{\sigma_j}(x_j)} \middle| x_j \right\} = o(1)$. It follows from (C.14) and (C.15) that

$$\begin{aligned} & h_x^{-1} - 2h_x^{-1} \mathbb{E} \left\{ \frac{\hat{f}_{\sigma_j}^{*,(j)}(x_j)}{f_{\sigma_j}(x_j)} \middle| x_j \right\} + h_x^{-1} \mathbb{E} \left\{ \frac{\hat{f}_{\sigma_j}^{*,(j)}(x_j)}{f_{\sigma_j}(x_j)} \middle| x_j \right\}^2 \\ &= O \left\{ h_x + \sup \sum_{k=1}^{\infty} \frac{1}{k!} \left(\frac{h_x^{2k-1} c^k x^{2k}}{2^k (\sigma^2 + h_x^2 c)^k} \right) \right\} + o(1). \end{aligned} \quad (\text{C.16})$$

By condition (C2) and the range of x , the RHS goes to 0.

Let $S_j = \sum_{i=1}^m \phi_{h_\sigma}(\sigma_j - \sigma_i)$ and $S_j^- = \sum_{i \neq j}^m \phi_{h_\sigma}(\sigma_j - \sigma_i)$. Some algebra shows $\hat{f}_{\sigma_j}^*(x_j) = \frac{S_j^-}{S_j} \hat{f}_{\sigma_j}^{*,(j)}(x_j) + \frac{1}{2S_j \pi h_\sigma h_x \sigma_j}$. We use the fact that $f_{\sigma_j}(x_j) \geq C_3 m^{-\delta/2}$ for some constant C_3 and Condition (C3) to claim that on \mathcal{A}^* ,

$$h_x^{-1} \frac{\mathbb{E}\{\hat{f}_{\sigma_j}^*(x_j) | x_j\}}{f_{\sigma_j}(x_j)} = h_x^{-1} \frac{\mathbb{E}\{\hat{f}_{\sigma_j}^{*,(j)}(x_j) | x_j\}}{f_{\sigma_j}(x_j)} + o(1). \quad (\text{C.17})$$

Similar computation shows that

$$h_x^{-1} \mathbb{E} \left\{ \frac{\hat{f}_{\sigma_j}^*(x_j)}{f_{\sigma_j}(x_j)} \middle| x_j \right\}^2 = h_x^{-1} \mathbb{E} \left\{ \frac{\hat{f}_{\sigma_j}^{*,(j)}(x_j)}{f_{\sigma_j}(x_j)} \middle| x_j \right\}^2 + o(1). \quad (\text{C.18})$$

(C.16), (C.17) and (C.18) together implies $h_x^{-1} h_\sigma^2 \mathbb{E}\{a_j^2 | x_j\} \rightarrow 0$. Hence $\mathbb{E} \int \left\{ \hat{f}_{1,\sigma}(x) - \tilde{f}_{1,\sigma}(x) \right\}^2 dx \rightarrow 0$ and Step (c) is established.

D Proof of Lemmas

D.1 Proof of lemma 1

Using the definitions of \hat{U}_i and U_i , we can show that $\left(\hat{U}_i - U_i \right)^2 = \left(\hat{T}_i - T_i \right)^2 \mathbb{I} \left(\hat{T}_i \leq t, T_i \leq t \right) + \left(\hat{T}_i - \alpha \right)^2 \mathbb{I} \left(\hat{T}_i \leq t, T_i > t \right) + (T_i - \alpha)^2 \mathbb{I} \left(\hat{T}_i > t, T_i \leq t \right)$. Denote the three sums on the RHS as I , II , and III respectively. By Proposition 2, $\mathbb{E}(I) = o(1)$. Let $\varepsilon > 0$. Consider

$$\begin{aligned} P \left(\hat{T}_i \leq t, T_i > t \right) &\leq P \left(\hat{T}_i \leq t, T_i \in (t, t + \varepsilon) \right) + P \left(\hat{T}_i \leq t, T_i \geq t + \varepsilon \right) \\ &\leq P \{ T_i \in (t, t + \varepsilon) \} + P (|T_i - T_i| > \varepsilon) \end{aligned}$$

The first term on the right hand is vanishingly small as $\varepsilon \rightarrow 0$ because \widehat{T}_{OR}^i is a continuous random variable. The second term converges to 0 by Proposition 2. we conclude that $II = o(1)$. In a similar fashion, we can show that $III = o(1)$, thus proving the lemma.

D.2 Proof of lemma 2

Note that $\mathbb{E}_{\boldsymbol{\theta}|\boldsymbol{\sigma},\mathbf{x}}(Y|\theta_j = 0) \geq \mathbb{E}_{\boldsymbol{\theta}|\boldsymbol{\sigma},\mathbf{x}}Y \geq \mathbb{E}_{\boldsymbol{\theta}|\boldsymbol{\sigma},\mathbf{x}}(Y|\theta_j = 1)$. It is sufficient to bound $\mathbb{E}_{\boldsymbol{\theta}|\boldsymbol{\sigma},\mathbf{x}}(Y|\theta_j = 0) - \mathbb{E}_{\boldsymbol{\theta}|\boldsymbol{\sigma},\mathbf{x}}(Y|\theta_j = 1)$. The lemma follows by noting that

$$\begin{aligned} & \mathbb{E}_{\boldsymbol{\theta}|\boldsymbol{\sigma},\mathbf{x}}(Y|\theta_j = 0) - \mathbb{E}_{\boldsymbol{\theta}|\boldsymbol{\sigma},\mathbf{x}}(Y|\theta_j = 1) \\ = & \mathbb{E}_{\boldsymbol{\theta}|\boldsymbol{\sigma},\mathbf{x}} \left\{ \frac{\phi_{h_\sigma}(\sigma - \sigma_j)}{\sum_{i \neq j} \phi_{h_\sigma}(\sigma - \sigma_i)\theta_i} \right\} - \mathbb{E}_{\boldsymbol{\theta}|\boldsymbol{\sigma},\mathbf{x}} \left\{ \frac{\phi_{h_\sigma}(\sigma - \sigma_j)}{\sum_{i \neq j} \phi_{h_\sigma}(\sigma - \sigma_i)\theta_i + \phi_{h_\sigma}(\sigma - \sigma_j)} \right\} \\ = & \mathbb{E}_{\boldsymbol{\theta}|\boldsymbol{\sigma},\mathbf{x}} \left\{ \frac{\phi_{h_\sigma}^2(\sigma - \sigma_j)}{\{\sum_{i \neq j} \phi_{h_\sigma}(\sigma - \sigma_i)\theta_i\} \{\sum_{i \neq j} \phi_{h_\sigma}(\sigma - \sigma_i)\theta_i + \phi_{h_\sigma}(\sigma - \sigma_j)\}} \right\} \\ \leq & \mathbb{E}_{\boldsymbol{\theta}|\boldsymbol{\sigma},\mathbf{x}} \left\{ \frac{\phi_{h_\sigma}^2(\sigma - \sigma_j)}{(\sum_{i \neq j} \phi_{h_\sigma}(\sigma - \sigma_i)\theta_i)^2} \right\} = O(m^{-2}). \end{aligned}$$

D.3 Proof of lemma 3

Let $Z = \sum_{i=1}^m \phi_{h_\sigma}(\sigma - \sigma_i)\mathbb{I}(\theta_i = 1)$, We expand $\frac{1}{Z}$ around $\mathbb{E}_{\boldsymbol{\theta}|\boldsymbol{\sigma},\mathbf{x}}(Z)$ and take expected value:

$$\mathbb{E}_{\boldsymbol{\theta}|\boldsymbol{\sigma},\mathbf{x}}\left(\frac{1}{Z}\right) = \mathbb{E}_{\boldsymbol{\theta}|\boldsymbol{\sigma},\mathbf{x}} \left[\frac{1}{\mathbb{E}_{\boldsymbol{\theta}|\boldsymbol{\sigma},\mathbf{x}}(Z)} - \frac{1}{\{\mathbb{E}_{\boldsymbol{\theta}|\boldsymbol{\sigma},\mathbf{x}}(Z)\}^2} (Z - \mathbb{E}_{\boldsymbol{\theta}|\boldsymbol{\sigma},\mathbf{x}}Z) + \sum_{k=3}^{\infty} \frac{(-1)^{k-1}}{\{\mathbb{E}_{\boldsymbol{\theta}|\boldsymbol{\sigma},\mathbf{x}}(Z)\}^k} (Z - \mathbb{E}_{\boldsymbol{\theta}|\boldsymbol{\sigma},\mathbf{x}}Z)^{k-1} \right].$$

The series converges on \mathcal{A} . Moreover, using normal approximation of binomial distribution, it can be shown that $\mathbb{E}_{\boldsymbol{\theta}|\boldsymbol{\sigma},\mathbf{x}}(Z - \mathbb{E}_{\boldsymbol{\theta}|\boldsymbol{\sigma},\mathbf{x}}Z)^k = O(m^{k/2})$. The lemma follows by noting that $\mathbb{E}_{\boldsymbol{\theta}|\boldsymbol{\sigma},\mathbf{x}}(Z^{-1}) = \{\mathbb{E}_{\boldsymbol{\theta}|\boldsymbol{\sigma},\mathbf{x}}(Z)\}^{-1} + O(m^{-2})$.

D.4 Proof of lemma 4

Consider $b_j^* = \frac{\phi_{h_\sigma}(\sigma - \sigma_j)\mathbb{I}(\theta_j = 1)}{\sum_{i=1}^m \phi_{h_\sigma}(\sigma - \sigma_i)\mathbb{I}(\theta_i = 1)}$ defined in Section C.1. Let $\tilde{b}_j = \frac{\theta_j}{\sum_{i=1}^m \theta_i}$. By Condition (C1), $Cov(b_j^*, b_k^*|\boldsymbol{\sigma}, \mathbf{x}) = O\{Cov(\tilde{b}_j, \tilde{b}_k|\boldsymbol{\sigma}, \mathbf{x})\}$. Note that $Cov(\tilde{b}_j, \tilde{b}_k|\boldsymbol{\sigma}, \mathbf{x}) = \mathbb{E}_{\boldsymbol{\theta}|\boldsymbol{\sigma},\mathbf{x}}(\tilde{b}_j\tilde{b}_k) - \mathbb{E}_{\boldsymbol{\theta}|\boldsymbol{\sigma},\mathbf{x}}(\tilde{b}_j)\mathbb{E}_{\boldsymbol{\theta}|\boldsymbol{\sigma},\mathbf{x}}(\tilde{b}_k)$. Using similar argument as in the proof for (C.12), we

have

$$\mathbb{E}_{\boldsymbol{\theta}|\boldsymbol{\sigma},\mathbf{x}}(\tilde{b}_j) = \frac{P(\theta_j = 1|\boldsymbol{\sigma},\mathbf{x})}{\sum_{i=1}^m P(\theta_i = 1|\boldsymbol{\sigma},\mathbf{x})} + O(m^{-2}) \text{ and } \mathbb{E}_{\boldsymbol{\theta}|\boldsymbol{\sigma},\mathbf{x}}(\tilde{b}_k) = \frac{P(\theta_k = 1|\boldsymbol{\sigma},\mathbf{x})}{\sum_{i=1}^m P(\theta_i = 1|\boldsymbol{\sigma},\mathbf{x})} + O(m^{-2}).$$

$$\text{It follows that } \mathbb{E}_{\boldsymbol{\theta}|\boldsymbol{\sigma},\mathbf{x}}(\tilde{b}_j)\mathbb{E}_{\boldsymbol{\theta}|\boldsymbol{\sigma},\mathbf{x}}(\tilde{b}_k) = \left\{ \frac{P(\theta_j = 1|\boldsymbol{\sigma},\mathbf{x})}{\sum_{i=1}^m P(\theta_i = 1|\boldsymbol{\sigma},\mathbf{x})} \right\} \left\{ \frac{P(\theta_k = 1|\boldsymbol{\sigma},\mathbf{x})}{\sum_{i=1}^m P(\theta_i = 1|\boldsymbol{\sigma},\mathbf{x})} \right\} + O(m^{-3}).$$

$$\text{Next we compute } \mathbb{E}_{\boldsymbol{\theta}|\boldsymbol{\sigma},\mathbf{x}}(\tilde{b}_j\tilde{b}_k). \text{ Note that } \mathbb{E}_{\boldsymbol{\theta}|\boldsymbol{\sigma},\mathbf{x}}(\tilde{b}_j\tilde{b}_k) = P(\theta_j = 1|\boldsymbol{\sigma},\mathbf{x})\mathbb{E}_{\boldsymbol{\theta}|\boldsymbol{\sigma},\mathbf{x}}\left\{ \frac{\theta_k}{(\sum_{i=1}^m \theta_i)^2} \middle| \theta_j = 1 \right\}.$$

$$\text{Using similar arguments as the proof for (C.11), we have } \text{Cov}\left\{ \theta_k, \frac{1}{(\sum_{i=1}^m \theta_i)^2} \middle| \theta_j = 1, \boldsymbol{\sigma}, \mathbf{x} \right\} = O(m^{-3}). \text{ Let } \boldsymbol{\theta}_{-k} = (\theta_j : 1 \leq j \leq m, j \neq k). \text{ We have}$$

$$\mathbb{E}_{\boldsymbol{\theta}|\boldsymbol{\sigma},\mathbf{x}}\left\{ \frac{\theta_k}{(\sum_{i=1}^m \theta_i)^2} \middle| \theta_j = 1 \right\} = P(\theta_k = 1|\boldsymbol{\sigma},\mathbf{x})\mathbb{E}_{\boldsymbol{\theta}_{-k}}\left\{ \frac{1}{(\sum_{i=1}^m \theta_i)^2} \middle| \theta_j = 1, \boldsymbol{\sigma}, \mathbf{x} \right\} + O(m^{-3}).$$

Using similar arguments in Lemmas 3 and 2, we have

$$\mathbb{E}_{\boldsymbol{\theta}_{-k}}\left\{ \frac{1}{(\sum_{i=1}^m \theta_i)^2} \middle| \theta_j = 1, \boldsymbol{\sigma}, \mathbf{x} \right\} = \frac{1}{\mathbb{E}_{\boldsymbol{\theta}|\boldsymbol{\sigma},\mathbf{x}}(\sum_{i=1}^m \theta_i)^2} + O(m^{-3}).$$

In the previous equation, the conditional expectation $\mathbb{E}_{\boldsymbol{\theta}_{-k}}$ can be replaced by $\mathbb{E}_{\boldsymbol{\theta}}$ because the term θ_k only affects the ratio by a term of order $O(m^{-3})$. Note that $\mathbb{E}_{\boldsymbol{\theta}|\boldsymbol{\sigma},\mathbf{x}}(\sum_{i=1}^m \theta_i)^2 = \{\mathbb{E}_{\boldsymbol{\theta}|\boldsymbol{\sigma},\mathbf{x}}(\sum_{i=1}^m \theta_i)\}^2 + \text{Var}(\sum_{i=1}^m \theta_i|\boldsymbol{\sigma},\mathbf{x})$ and $\text{Var}(\sum_{i=1}^m \theta_i|\boldsymbol{\sigma},\mathbf{x}) \leq m$. We have

$$\mathbb{E}_{\boldsymbol{\theta}|\boldsymbol{\sigma},\mathbf{x}}\left\{ \frac{\theta_k}{(\sum_{i=1}^m \theta_i)^2} \middle| \theta_j = 1 \right\} = \frac{P(\theta_k = 1|\boldsymbol{\sigma},\mathbf{x})}{\{\sum_{i=1}^m P(\theta_i = 1|\boldsymbol{\sigma},\mathbf{x})\}^2} + O(m^{-3}).$$

Finally, the lemma follows from the fact that

$$\text{Cov}(\tilde{b}_j, \tilde{b}_k|\boldsymbol{\sigma}, \mathbf{x}) = \mathbb{E}_{\boldsymbol{\theta}|\boldsymbol{\sigma},\mathbf{x}}(\tilde{b}_j\tilde{b}_k) - \mathbb{E}_{\boldsymbol{\theta}|\boldsymbol{\sigma},\mathbf{x}}(\tilde{b}_j)\mathbb{E}_{\boldsymbol{\theta}|\boldsymbol{\sigma},\mathbf{x}}(\tilde{b}_k) = O(m^{-3}).$$